

NASA/TM—2011–216454



# Notes on Lithology, Mineralogy, and Production for Lunar Simulants

*D.L. Rickman*

*Marshall Space Flight Center, Marshall Space Flight Center, Alabama*

*D.B. Stoeser and W.M. Benzel*

*United States Geological Survey Denver Federal Center, Denver, Colorado*

*C.M. Schrader*

*Oak Ridge Associated Universities, Oak Ridge, Tennessee*

*J.E. Edmunson*

*BAE Systems, Huntsville, Alabama*

---

*January 2011*

## The NASA STI Program...in Profile

Since its founding, NASA has been dedicated to the advancement of aeronautics and space science. The NASA Scientific and Technical Information (STI) Program Office plays a key part in helping NASA maintain this important role.

The NASA STI Program Office is operated by Langley Research Center, the lead center for NASA's scientific and technical information. The NASA STI Program Office provides access to the NASA STI Database, the largest collection of aeronautical and space science STI in the world. The Program Office is also NASA's institutional mechanism for disseminating the results of its research and development activities. These results are published by NASA in the NASA STI Report Series, which includes the following report types:

- **TECHNICAL PUBLICATION.** Reports of completed research or a major significant phase of research that present the results of NASA programs and include extensive data or theoretical analysis. Includes compilations of significant scientific and technical data and information deemed to be of continuing reference value. NASA's counterpart of peer-reviewed formal professional papers but has less stringent limitations on manuscript length and extent of graphic presentations.
- **TECHNICAL MEMORANDUM.** Scientific and technical findings that are preliminary or of specialized interest, e.g., quick release reports, working papers, and bibliographies that contain minimal annotation. Does not contain extensive analysis.
- **CONTRACTOR REPORT.** Scientific and technical findings by NASA-sponsored contractors and grantees.
- **CONFERENCE PUBLICATION.** Collected papers from scientific and technical conferences, symposia, seminars, or other meetings sponsored or cosponsored by NASA.
- **SPECIAL PUBLICATION.** Scientific, technical, or historical information from NASA programs, projects, and mission, often concerned with subjects having substantial public interest.
- **TECHNICAL TRANSLATION.** English-language translations of foreign scientific and technical material pertinent to NASA's mission.

Specialized services that complement the STI Program Office's diverse offerings include creating custom thesauri, building customized databases, organizing and publishing research results...even providing videos.

For more information about the NASA STI Program Office, see the following:

- Access the NASA STI program home page at <http://www.sti.nasa.gov>
- E-mail your question via the Internet to [help@sti.nasa.gov](mailto:help@sti.nasa.gov)
- Fax your question to the NASA STI Help Desk at 443-757-5803
- Phone the NASA STI Help Desk at 443-757-5802
- Write to:  
NASA STI Help Desk  
NASA Center for AeroSpace Information  
7115 Standard Drive  
Hanover, MD 21076-1320

NASA/TM—2011–216454



# Notes on Lithology, Mineralogy, and Production for Lunar Simulants

*D.L. Rickman*

*Marshall Space Flight Center, Marshall Space Flight Center, Alabama*

*D.B. Stoeser and W.M. Benzel*

*United States Geological Survey Denver Federal Center, Denver, Colorado*

*C.M. Schrader*

*Oak Ridge Associated Universities, Oak Ridge, Tennessee*

*J.E. Edmunson*

*BAE Systems, Huntsville, Alabama*

National Aeronautics and  
Space Administration

Marshall Space Flight Center • MSFC, Alabama 35812

---

*January 2011*

Available from:

NASA Center for AeroSpace Information  
7115 Standard Drive  
Hanover, MD 21076-1320  
443-757-5802

This report is also available in electronic form at  
<<https://www2.sti.nasa.gov>>



## TABLE OF CONTENTS

1. IGNEOUS ROCK NAMES .....	1
1.1 International Union of Geological Sciences Classification .....	1
1.2 Lunar Lithologic Terminology .....	6
1.3 Impactite Classification .....	8
2. PYROXENES .....	10
2.1 Pyroxene Melting Phase Equilibria for In Situ Resource Utilization .....	12
3. PLAGIOCLASE .....	16
3.1 Plagioclase Melting Phase Equilibria for In Situ Resource Utilization .....	18
4. OLIVINE .....	20
4.1 Olivine Melting Phase Equilibria for In Situ Resource Utilization .....	21
5. REGOLITH SIMULANT NAMING PROTOCOL .....	22
5.1 Scope .....	22
5.2 Objective .....	22
5.3 Justification .....	22
5.4 Protocol .....	22
5.5 Configuration Management .....	24
5.6 Contact Information .....	24
6. MINERAL SEPARATES .....	25
6.1 Justification .....	25
6.2 Terminology .....	25
6.3 Evaluation Criteria .....	26
6.4 Feedstock Description: Stillwater Norite .....	27
6.5 Technical Results of Mineral Separation Test .....	30
6.6 Eriez Manufacturing Co. ....	36
6.7 Analysis .....	42
6.8 Bushveld .....	43
REFERENCES .....	47

## LIST OF FIGURES

1.	Basic classification of crystalline igneous rocks. See text for explanation. Redrawn from reference 1 .....	3
2.	Rock names depending on the relative abundance of plagioclase, pyroxene, and olivine. Conceptually, this is an elaboration of the diorite/gabbro/anorthosite field in figure 1. Redrawn from reference 1 .....	4
3.	Rock names depending on the relative abundance of plagioclase, clinopyroxene, and orthopyroxene. Conceptually, this is an elaboration of the gabbro, gabbro-norite, and norite field of figure 2. Redrawn from reference 1 .....	4
4.	Rock names depending on the relative abundance of plagioclase, clinopyroxene, and orthopyroxene. Conceptually, this is an elaboration of the ultramafic field of figure 2. Redrawn from reference 1 .....	5
5.	Classification of rocks made from particles expelled by a volcanic eruption. Redrawn from reference 1 .....	5
6.	Classification of volcanic rock based on the relative abundance of silicon, sodium, and potassium. Redrawn from reference 1 .....	6
7.	Sensu lato lithologic lunar terminology for the px-plag-ol modal ternary diagram (adapted from reference 4). Compare to figure 2 .....	7
8.	Classification of lunar highlands rocks based on plagioclase, orthopyroxene, and clinopyroxene content after reference 4. Compare to figure 3 .....	8
9.	Classification of impactites after reference 6. Note that this is a general classification and not strictly for lunar impactites .....	9
10.	Pyroxene Ca-Mg-Fe quadrilateral showing mineral names and approximate range of lunar pyroxenes according to reference 14 .....	10
11.	The variation in melting point, Mohs hardness, specific gravity, and cleavage of pyroxenes in the pyroxene Ca-Mg-Fe quadrilateral .....	11
12.	Pyroxene compositions in Apollo 16 (highlands) regolith samples .....	11
13.	Pyroxene compositions in Apollo 11, 12, 14, 15, and 17 mare basalt samples .....	12

## LIST OF FIGURES (Continued)

14.	Composition of Stillwater pyroxenes (see section 6.4). .....	12
15.	Pyroxene phase relations from experiments on natural terrestrial and lunar pyroxenes at 1 bar and low-oxygen fugacity. Redrawn from reference 18. Liquidus diagram (a), and solidus diagram (b) .....	14
16.	Solidus diagram from figure 15. The same symbols apply. The light-gray shading indicates the silica-bearing field. The blue field delineates analyzed lunar highland pyroxene compositions. The area where the two fields overlap may indicate compositions where tridymite, cristobalite, or other silicon dioxide phases may be encountered during melting .....	15
17.	Feldspar ternary diagram denoting the compositional ranges of feldspars. Original diagram redrawn from reference 11. Lunar plagioclase data from reference 19 .....	16
18.	Plagioclase composition histogram for the Apollo 16 site, dominated by ferroan anorthosites. Note the high molar percentage of Ca in the plagioclase structure (denoted by modal percent An). Data compiled from reference 16 and other sources .....	17
19.	Plagioclase compositions in mare basalts where An indicates molar percentage of Ca in the plagioclase structure .....	18
20.	Feldspar ternary diagram indicating possible stable compositional ranges of feldspars with different temperatures and pressures of solidification. Diagram redrawn from reference 11 after reference 22 .....	19
21.	Plagioclase binary diagram, indicating solidus and liquidus temperatures for anhydrous conditions (top) and 5-kbar H <sub>2</sub> O conditions (bottom). The highlighted area indicates compositions of lunar plagioclase. Note that evidence suggests anhydrous conditions for the formation of lunar rocks .....	19
22.	Olivine compositions from Apollo 16 regolith samples. Data compiled from reference 16 and other sources .....	20
23.	Mare basalt olivine compositions from Apollo missions 11, 12, 15, and 17, with data from Luna 16 and Luna 24. Data compiled from reference 25 and other sources .....	21
24.	Solidus (bottom) and liquidus (top) temperatures for the Fo-fayalite solid solution at 1 bar pressure. Redrawn from reference 26 .....	21

## LIST OF FIGURES (Continued)

25.	Road norite .....	28
26.	Detail from figure 25 .....	28
27.	Norite after first stage crushing. Note the wide range in color variation. This is a result of both variations in the relative abundance of pyroxenes and the amount of hydrothermal alteration .....	29
28.	Thin section of Stillwater norite in plane-polarized, transmitted light. Detailed examination shows traces of alteration minerals disseminated in the pyroxenes .....	29
29.	Same view as in figure 28 but under crossed nicols. In this thin section, the ‘smudgy’ appearance of the pyroxenes (e.g., the orthopyroxene grain in the upper left) is indicative of alteration minerals .....	30
30.	Flow diagram for 10–35-mesh particles from Stillwater norite by magnetic separation. Work done by Hazen Research, Inc. ....	32
31.	Flow diagram for 35–100-mesh particles from Stillwater norite by magnetic separation. Work done by Hazen Research, Inc. ....	32
32.	The concentrate 32(a) and tails 32(b) from the 10–35-mesh fraction as processed according to figure 30 .....	34
33.	The concentrate 33(a) and tails 33(b) from the 35–100-mesh fraction as processed according to figure 31. The photo of the tails in figure 33(b) shows marked segregation of colors .....	34
34.	The basic theory of operation of a belt-driven, rare-earth, magnetic separator .....	37
35.	First pass process flow used by Eriez. Compare with figures 31 and 32. The differences reflect the different processing objectives of the work at Hazen and the work at Eriez .....	38
36.	Second pass process flow used by Eriez. Because the feedstock for this process came from the magnetic fraction obtained from the preceding process, even splits 6 and 8 are distinctly magnetic compared to plagioclase .....	39
37.	A conceptual rearrangement of the preceding processing flow diagrams suggested by Eriez .....	40

## LIST OF FIGURES (Continued)

38.	Impala Black in plane-polarized, transmitted light (clinopyroxene and plagioclase) .....	44
39.	Same view as in figure 38 but under crossed nicols. Compare with figures 28 and 29 .....	44
40.	A quarry that produces the dimension stone Impala Black. This is but one of many quarries operated by M+Q and producing this specific stone. Image by Jonathan Houghton .....	45
41.	Working faces in quarry shown in figure 40. Almost all of the rock in view is functionally identical for the purposes of simulant utility. Image by Jonathan Houghton .....	46

## LIST OF TABLES

1.	Maximum* particle size name scheme .....	23
2.	Magnetic susceptibilities of the major minerals of the road norite .....	31
3.	The relationship between mesh number and particle size in microns .....	31
4.	Yields of the processes in flow diagrams in figures 30 and 31 .....	33
5.	Cost estimates for processing 1 ton of road norite per the flow diagrams shown in figures 30 and 31 .....	36
6.	XRD instrument description used for analysis of mineral separates .....	40
7.	Modal mineralogy of selected splits from magnetic separations by Eriez .....	42

## LIST OF ACRONYMS, SYMBOLS, AND ABBREVIATIONS

Al	aluminum
An	anorthite
ANT	anorthosite, norite, and troctolite
Ba	barium
Ca	calcium
CIPW	Cross, Iddings, Pirsson, and Washington
cpx	clinopyroxene
Cr	chromium
Cu	copper
Di	diopside
En	enstatite
Eu	europium
Fe	iron
Fo	forsterite
Fs	ferrosilite
Hd	hedenbergite
ISRU	in situ resource utilization
IUGS	International Union of Geological Sciences
K	potassium
La	lanthanum
Li	lithium

## LIST OF ACRONYMS, SYMBOLS, AND ABBREVIATIONS (Continued)

Lu	lutetium
MDI	Material Data Inc.
Mg	magnesium
Mn	manganese
Na	sodium
Ni	nickel
NIST	National Institute of Standards and Technology
NU	National Aeronautics and Space Administration/United States Geological Survey
ol	olivine
opx	orthopyroxene
Orb	Orbitec
plag/pl	plagioclase
px	pyroxene
Rb	rubidium
Si	silicon
sl	sensu lato
Sr	strontium
Ti	titanium
U.S.	United States
USGS	United States Geological Survey
WPF	Whole Pattern Fit
XRD	X-ray diffraction



## TECHNICAL MEMORANDUM

### NOTES ON LITHOLOGY, MINERALOGY, AND PRODUCTION FOR LUNAR SIMULANTS

#### 1. IGNEOUS ROCK NAMES

For a geologist, the name a rock is given places it in a conceptual context. It is one, and possibly the most important, of the fundamental organizing principles in geology. Simply knowing the rock name says much about the rocks, including genesis, type of terrane, the mineralogy, particle or grain sizes, associated ores, weathering characteristics, and chemistry of the rock. Knowing the type of rock to be simulated provides a strong guide as to where and how to find similar rocks.

There were no recognized international standards for the naming of igneous rocks when Apollo first landed on the Moon. In 1975, the first such standard was published by the International Union of Geological Sciences (IUGS). Since then, revisions of this standard and a relevant standard for metamorphic rocks have been published and widely accepted.

##### **1.1 International Union of Geological Sciences Classification**

The figures and information in this section are extracted from or redrawn from the IUGS Subcommission on the Systematics of Igneous Rocks.<sup>1</sup> For a full discussion of these figures and their application please see reference 1. Reference 1 is the internationally accepted standard for the classification of plutonic rocks and volcanic rocks. Regrettably, much, if not most, of the literature about lunar lithologic composition does not use the international standard. Technical literature dealing with terrestrial material written since the middle 1970s does use either this standard or earlier editions of this standard.

The naming and classification of rocks is based on the relative proportions of specific mineral groups. The specific measurement is the volume modal abundance. Modal abundance is obtained by measuring the abundance of actual minerals. This is in contrast to normative abundance, which is obtained by computing presumed mineralogy based on chemical abundance.

Classification starts with figure 1. The mineral groups used in figure 1 are referred to as Q, A, P, F, and M. The following is extracted from section 2.1.1 of the standard:<sup>1</sup>

- “Q = quartz, tridymite, and cristobalite.
- A = alkali feldspar, including orthoclase, microcline, perthite, anorthoclase, sanidine, and albitic plagioclase (plag/pl) ( $An_0$  to  $An_5$ ).
- P = plagioclase ( $An_5$  to  $An_{100}$ ) and scapolite.
- F = feldspathoids or foids including nepheline, leucite, kalsilite, analcime, sodalite, nosean, haiiyne, cancrinite, and pseudoleucite.
- M = mafic and related minerals (e.g., mica, amphibole, pyroxene (px), olivine (ol), opaque minerals, accessory minerals (e.g., zircon, apatite, and titanite), epidote, allanite, garnet, melilite, monticellite, and primary carbonate).

Groups Q, A, P, and F comprise the felsic minerals, while the minerals of group M are considered to be mafic minerals, from the point of view of the modal classifications.”

The most common terrestrial, coarse-grained, igneous rocks fall in the center of the upper half of the diagram. There are abundant terrestrial occurrences within all fields of the diagram. Lunar crustal rocks almost exclusively lie within one field of the diagram, the diorite/gabbro/anorthosite field. Figure 2 expands this field. As the quartz, alkali feldspar, and feldspathoid groups are minor or absent from these rocks, the classification scheme evaluates the relative abundances of plagioclase, pyroxene, and olivine. Figure 3 further restricts consideration to just plagioclase, orthopyroxene (opx), and clinopyroxene (cpx). Figure 4 expands the ultramafic field of figure 2. Figures 1–4 cover intrusive rocks (i.e., rocks forming from molten material that never reaches the surface). These were formed by precipitation of crystalline phases directly from a molten source material in processes dominated by cooling. As a result of slow cooling, which has allowed crystals to grow relatively large, the individual phases are coarse enough to be identified with the aid of a hand lens.

Extrusive volcanic rocks (rocks that formed from molten material that reached the surface) cooled more rapidly than the intrusive rocks. As a result, glasses and crystalline material that are too fine in size to be confidently identified with only the aid of a hand lens dominate these rocks. In many cases, a volcanic eruption will violently expel material, forming isolated particles in the process. Figure 5 shows a classification of extrusive igneous rocks based on particle size. Figure 6 is relevant when dealing with extrusive volcanic rock that was not formed as the result of explosive processes, based on the relative abundance of silicon (Si), sodium (Na), and potassium (K).

There are complexities not addressed by these figures. For geologists, these provide a framework not a finale. Further, not all igneous rocks fall into these figures, but they are relevant to lunar crustal materials and therefore lunar simulants.

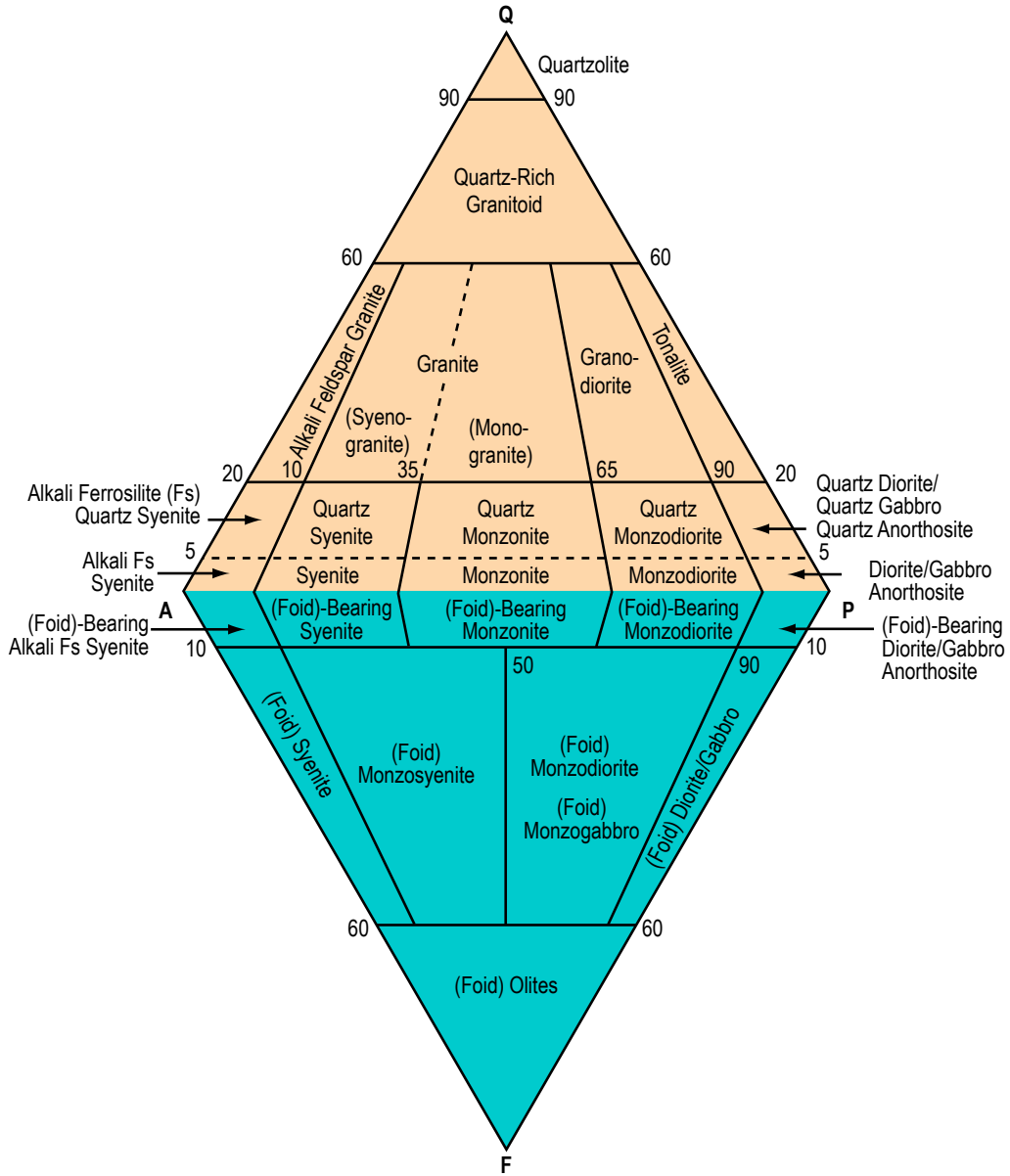


Figure 1. Basic classification of crystalline igneous rocks. See text for explanation. Redrawn from reference 1.

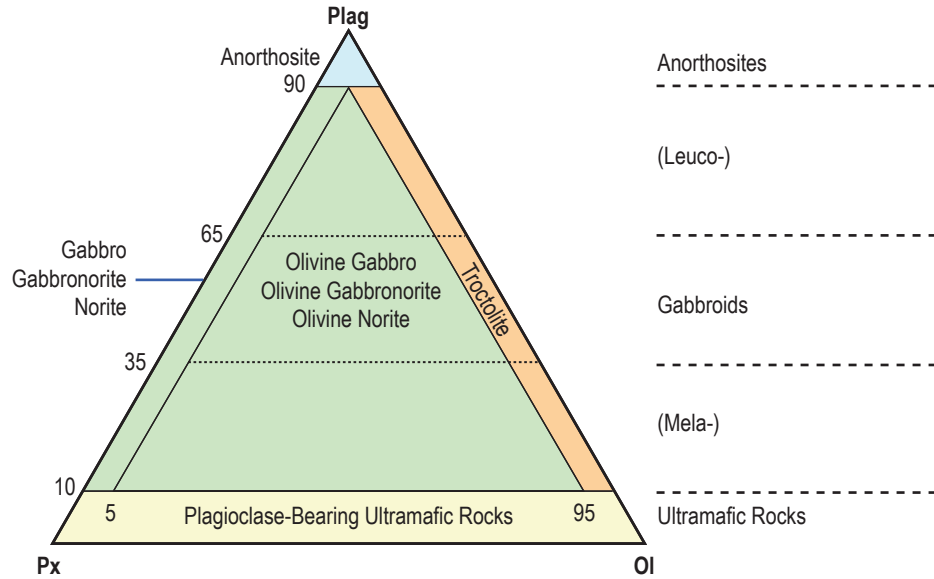


Figure 2. Rock names depending on the relative abundance of plagioclase, pyroxene, and olivine. Conceptually, this is an elaboration of the diorite/gabbro/anorthosite field in figure 1. Redrawn from reference 1.

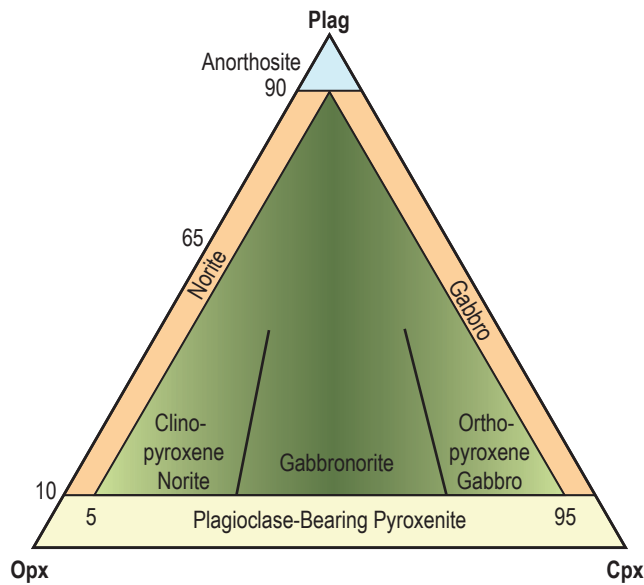


Figure 3. Rock names depending on the relative abundance of plagioclase, clinopyroxene, and orthopyroxene. Conceptually, this is an elaboration of the gabbro, gabbronorite, and norite field of figure 2. Redrawn from reference 1.

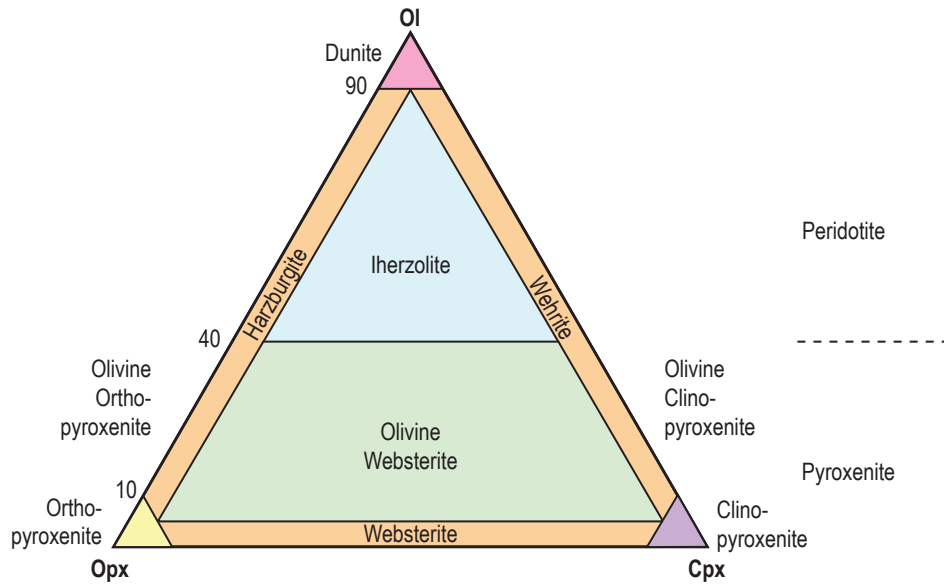


Figure 4. Rock names depending on the relative abundance of plagioclase, clinopyroxene, and orthopyroxene. Conceptually, this is an elaboration of the ultramafic field of figure 2. Redrawn from reference 1.

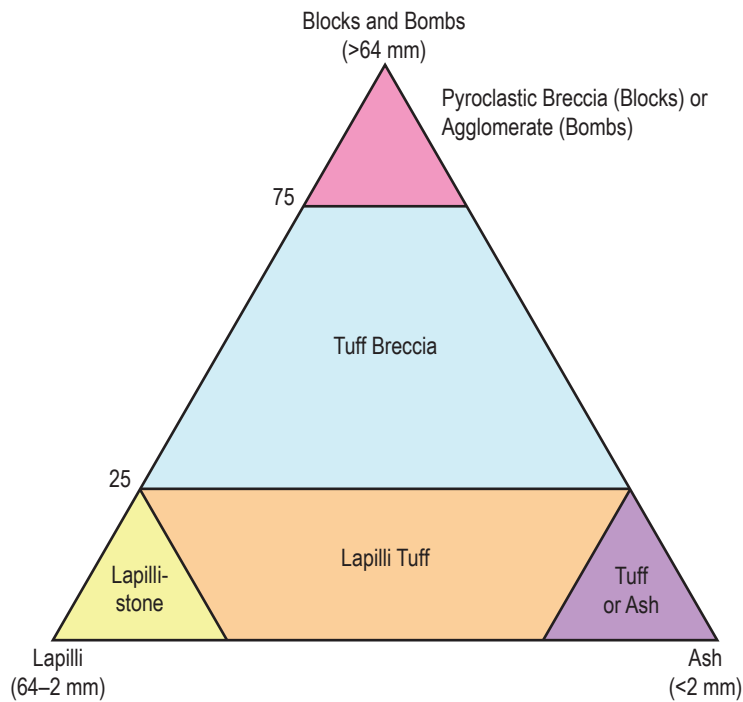


Figure 5. Classification of rocks made from particles expelled by a volcanic eruption. Redrawn from reference 1.

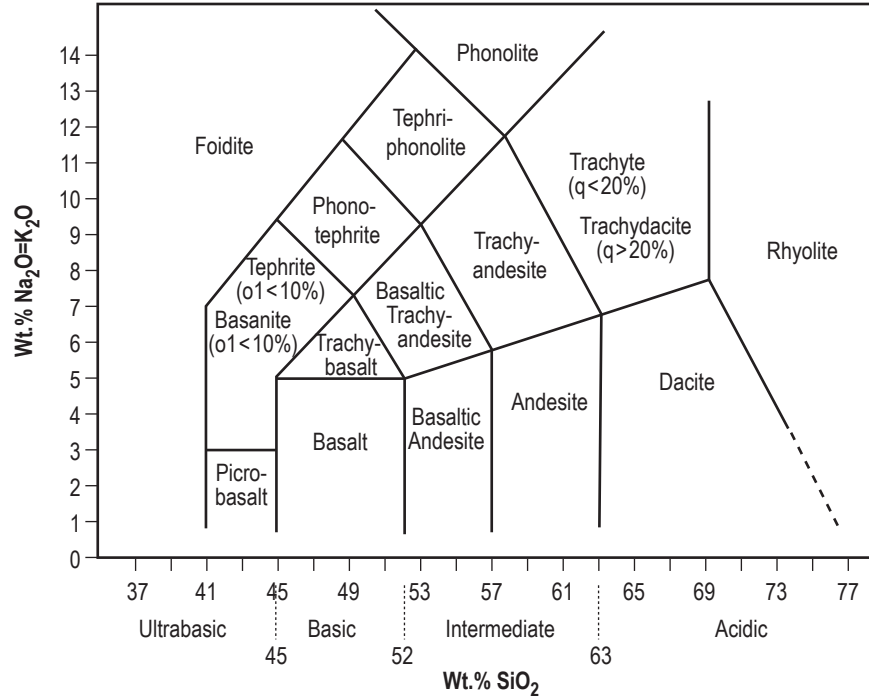


Figure 6. Classification of volcanic rock based on the relative abundance of Si, Na, and K. Redrawn from reference 1.

## 1.2 Lunar Lithologic Terminology

Although most terrestrial igneous rocks fit within the preceding naming scheme, lunar rocks are much more problematic. There are several reasons for this. First, the terminology used within the community of lunar geologists does not follow standard usage in many respects. This has been noted by various authors such as Ashwal,<sup>2</sup> and the point is made especially forcefully in reference 3. From page 140 of reference 3, emphasis added,

“A series of rocks commonly called the ANT suite composes most of the returned terra material, where ANT refers to the plutonic rock types anorthosite (min. 90 percent plagioclase), norite (plagioclase and orthopyroxene), and troctolite (plagioclase and olivine; table 8.1; Prinz and Keil, 1977; Stöffler and others, 1980). The plagioclase-rich composition of the terrae was first recognized in studies of small fragments in the Apollo 11 mare regolith (Wood, 1970; Wood and others, 1970), and the ANT suite was defined on the basis of small fragments in the Luna 16 and 20 regolith samples (Keil and others, 1972; Prinz and others, 1973; Taylor, G.J., and others, 1973; Prinz and Keil, 1977). Because the importance of impact mixing and melting was not fully appreciated during these early analyses, compositional types were commonly delineated incorrectly on the basis of mixed, brecciated, fine-grained, or even glassy rocks as if they were plutonic igneous rocks containing large optically identifiable crystals. The name ‘anorthosite’ has been especially misused for materials that are not anorthosites in either the compositional or textural sense.”

“In ANT terminology, the ‘average’ terra rock is an anorthositic norite or a noritic anorthosite (approx. 70 percent normative plagioclase; Taylor, 1975, 1982). Unfortunately for the nonspecialist, this composition is also referred to as ‘highland basalt.’ This term was coined during study of regolith glasses (Reid and others, 1972a) and is one of several terms containing the word ‘basalt’ that, especially in literature of the early 1970s, refer not to crystalline extrusive rocks but to magmas whose existence was predicted on the basis of glassy fragments (Apollo Soil Survey, 1971, 1974; Reid and others, 1972a, b; Prinz and others, 1973). Early workers commonly stated that ‘highland basalt’ represents the most important primary magma of the terrae.”

Regrettably, this failure to adopt the international standard has caused, and continues to cause, confusion for nonspecialists. There have been multiple attempts to standardize the naming conventions. One relatively successful attempt was by Stöffler et al.<sup>4</sup> Figures 7 and 8 show relevant portions of this scheme. However, debate on the basic naming logic for use with lunar rocks continues (e.g., reference 5). Part of the reluctance within the lunar geology community to using the standard names is historical and personal; and, to do so would cause an element of confusion within the literature of the community. But more importantly, the lunar rocks are not really just igneous rocks, at least not in the sense common for terrestrial rocks. They have been massively changed by hypervelocity impacts. It is fair to ask why geologists continue to name the lunar rocks based on what the rock was originally. Doing so is a universal practice for geologists.

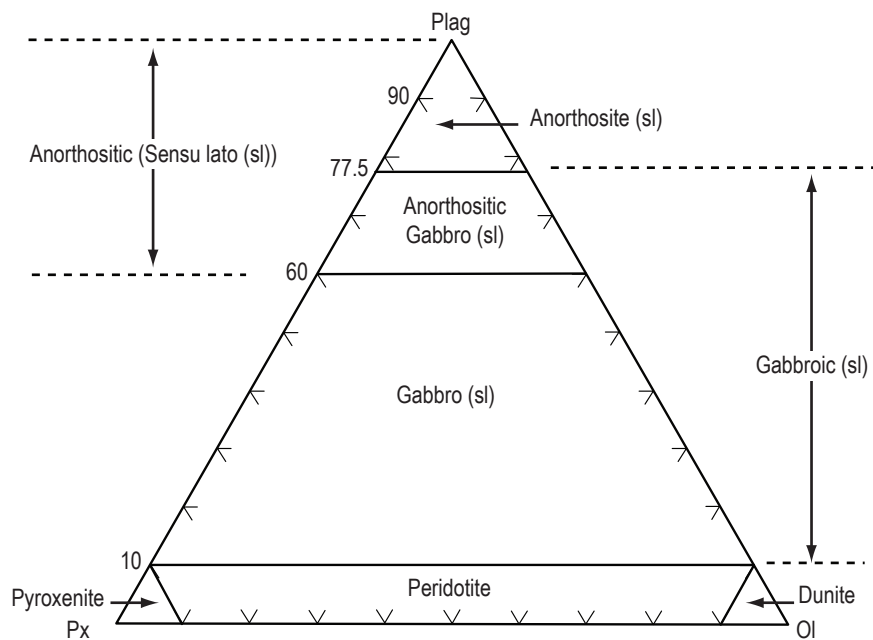


Figure 7. Sensu lato lithologic lunar terminology for the px–plag–ol modal ternary diagram (adapted from reference 4). Compare to figure 2.

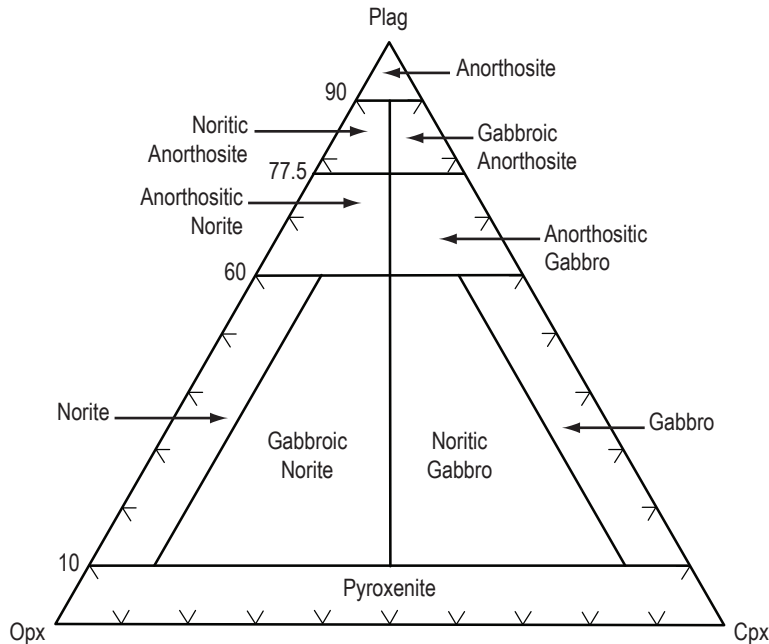


Figure 8. Classification of lunar highlands rocks based on plagioclase, orthopyroxene, and clinopyroxene content after reference 4. Compare to figure 3.

This is a point of confusion for nongeologists; however, a specific rock, outcrop, or road cut will commonly be given a lithologic name, but the actual material is most decidedly not that material. For example, geologic maps of the southeastern United States (U.S.) show bands of igneous and metamorphic rocks, but these crystalline rocks are not to be found where the bands are intersected by road cuts. Clays have replaced the actual stone through weathering; however, the original textures of the rock are readily evident. Weathering and other alteration processes are so wide spread and so complex that the only practical way to map the material is to base the map on what the rock was originally. Anyone who has ever studied soil maps will recognize the strength of this argument.

Thus, when the Apollo missions returned samples, the lunar geology community quickly recognized that the original rocks were igneous and, though the rocks were massively altered by impact, used igneous rock names to describe the material. But doing so ignores the very important role of the hypervelocity impacts in forming the geologic materials. To address this, a new type of rock has been defined within the metamorphic rocks. Reference 6 is the basic reference for the new rock definition. The recommendations in reference 6 are not without some points of contention such as those found in reference 7.

### 1.3 Impactite Classification

Impactite is a term for rock created or modified by the shock and thermal effects of an impact.<sup>6</sup> A classification scheme for impactites is shown in figure 9. Impactites can range from target rocks that are, to various degrees, modified by impact effects to rock formed by complete melting. For more information about lunar impactite classification see references 8, 9, and 10.



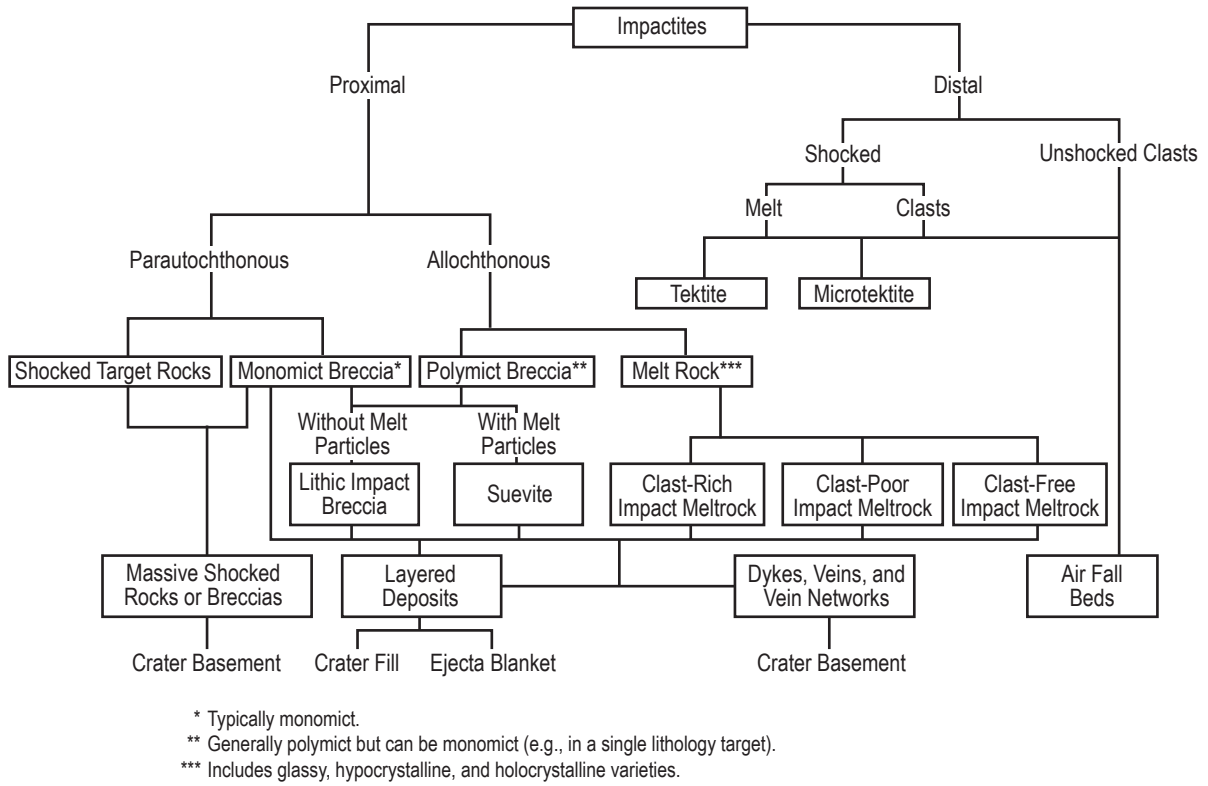


Figure 9. Classification of impactites after reference 6. Note that this is a general classification and not strictly for lunar impactites.

## 2. PYROXENES

Pyroxenes are the most abundant ferromagnesian silicate minerals on the Earth and the Moon. Pyroxene compositions fall largely into the subset of the ternary system  $\text{MgSiO}_3$ - $\text{CaSiO}_3$ - $\text{FeSiO}_3$  below 50 mole %  $\text{CaSiO}_3$ . This truncated ternary field is bounded by the compositions  $\text{CaMgSi}_2\text{O}_6$  (diopside (Di))- $\text{CaFeSi}_2\text{O}_6$  (hedenbergite (Hd))- $\text{MgSi}_2\text{O}_6$  (enstatite (En))- $\text{FeSi}_2\text{O}_6$  (ferrosilite (Fs)) and is known in mineralogical vernacular as the ‘pyroxene quadrilateral’ (fig. 10–16). Pyroxenes may also contain nontrivial amounts of other cations. For terrestrial pyroxenes, other cations present include  $\text{Na}^+$ ,  $\text{Li}^+$ ,  $\text{Mn}^{+2}$ ,  $\text{Fe}^{+3}$ ,  $\text{Al}^{+3}$ ,  $\text{Cr}^{+3}$ , and  $\text{Ti}^{+4}$ .<sup>11</sup> Usually, these are referred to as nonessential, as their presence or absence in normal amounts does not significantly affect the crystal lattice. However, they can become essential in some cases. For example, sodium can replace calcium almost completely, forming the pyroxene aegerine. In lunar pyroxenes, the nonessential cations are dominantly  $\text{Cr}^{+3}$ ,  $\text{Al}^{+3}$ , and  $\text{Ti}^{+4}$ , though  $\text{Cr}^{+2}$  and  $\text{Ti}^{+3}$  occur in subordinate amounts.<sup>12</sup>

Especially for lunar work, most pyroxene phase equilibria can be described qualitatively and quantitatively by the quadrilateral system. For simulant work, minerals in the aegerine to aegerine-augite compositional range should be avoided. A low-sodium augite, preferably with an  $\text{En}/(\text{En}+\text{Fs})$  ratio of around  $70 \pm 15$  is needed. This means that most terrestrial augites are acceptable.

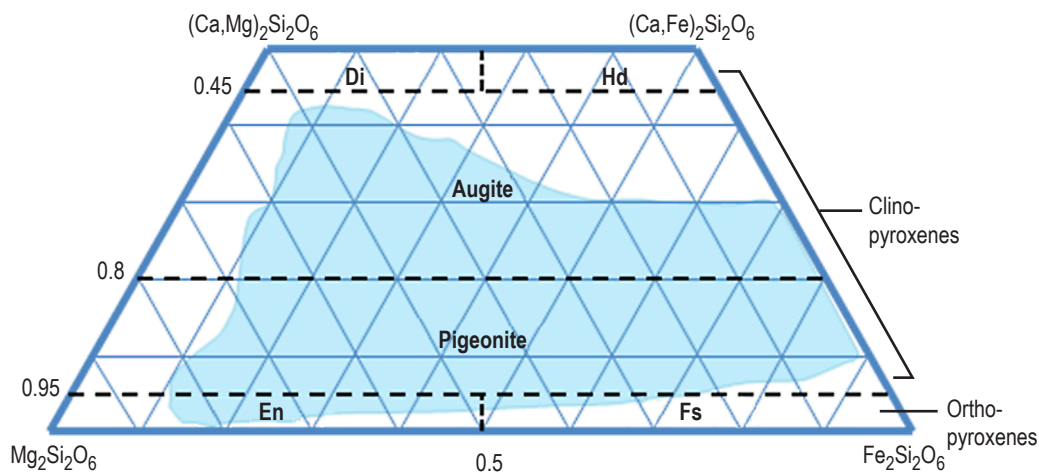


Figure 10. Pyroxene Ca-Mg-Fe quadrilateral showing mineral names<sup>13</sup> and approximate range of lunar pyroxenes according to reference 14.

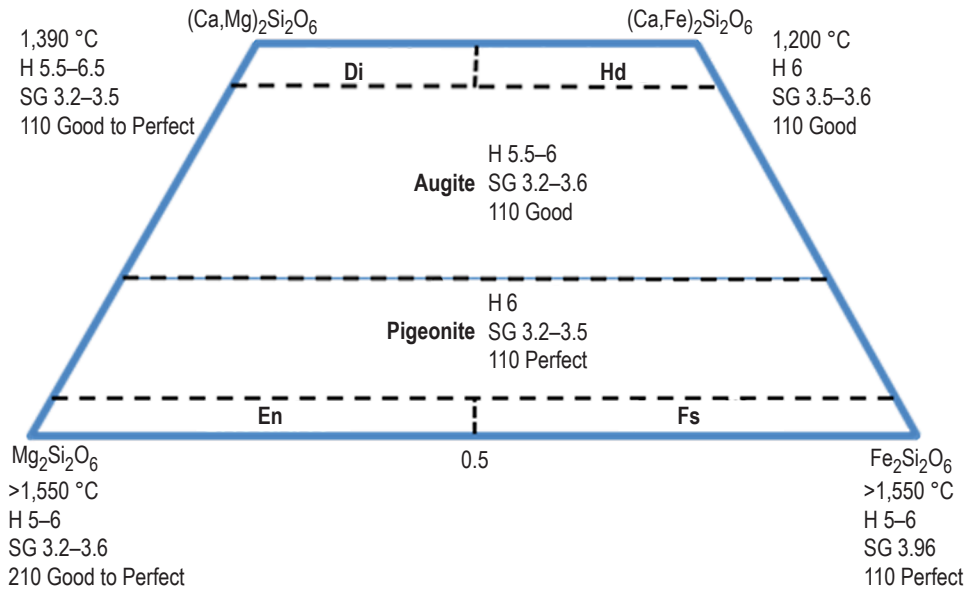


Figure 11. The variation in melting point, Mohs hardness, specific gravity, and cleavage of pyroxenes in the pyroxene Ca-Mg-Fe quadrilateral.<sup>15</sup>

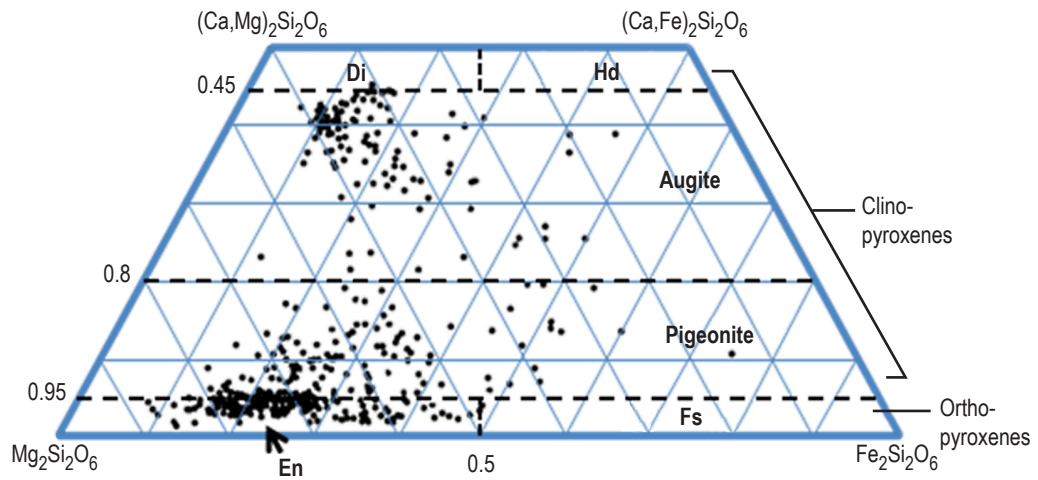


Figure 12. Pyroxene compositions in Apollo 16 (highlands) regolith samples.<sup>16</sup>

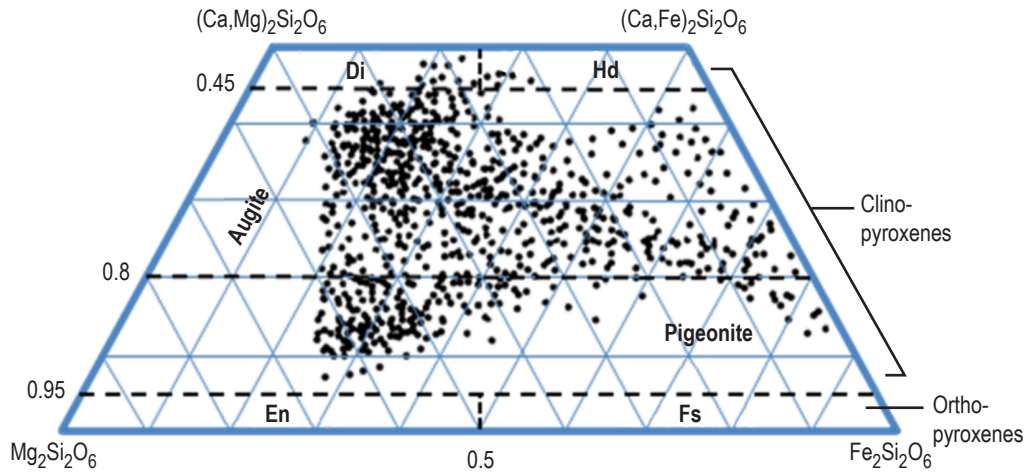


Figure 13. Pyroxene compositions in Apollo 11, 12, 14, 15, and 17 mare basalt samples.<sup>17</sup>

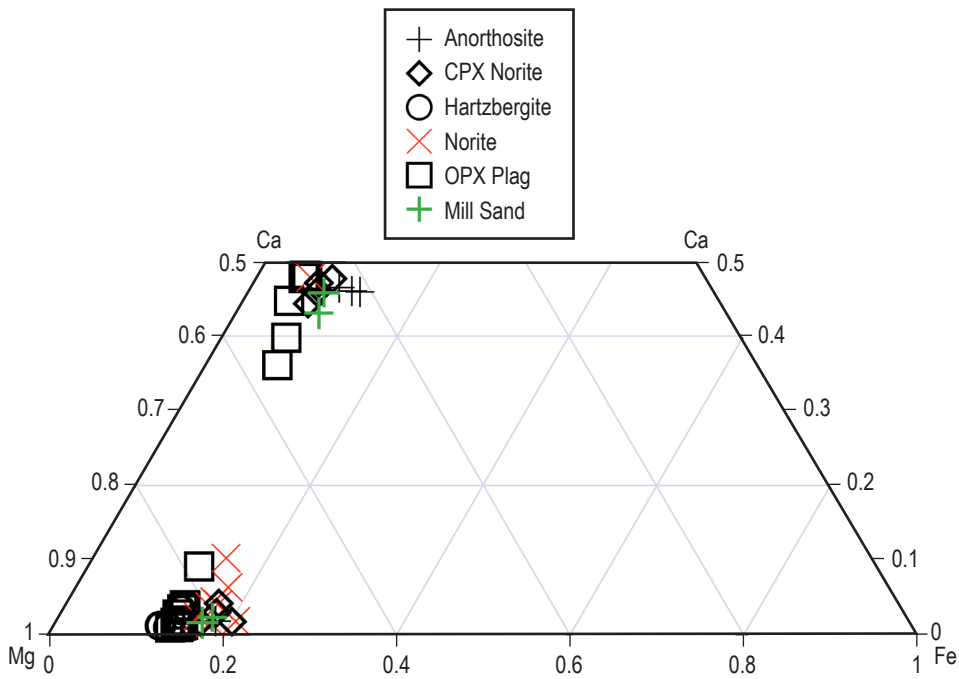


Figure 14. Composition of Stillwater pyroxenes (see section 6.4).

## 2.1 Pyroxene Melting Phase Equilibria for In Situ Resource Utilization

Many engineering activities for in situ resource utilization (ISRU), fabrication, etc., involve partial or total melting of lunar regolith or simulants. Melting of these materials occurs in a step-wise fashion as temperature increases and phases (minerals or glass) not present in the starting material may crystallize and melt during this process. Furthermore, some minerals may have

exsolved into multiple phases under terrestrial or lunar surface conditions, also leading to the presence of unexpected phases. To avoid possible problems, a documentation of possible melting phase equilibria is desirable.

There is an iron-rich portion of the pyroxene quadrilateral where olivine + silica are stable at the expense of pyroxene. Huebner and Turnock's experimentally derived plots (fig. 15) show these fields.<sup>18</sup> In some cases, a pyroxene (augite (A) or pigeonite (P)) is present on the solidus (fig. 15 (b)) but is joined by olivine (F) and silica (S). Figure 16 shows the outline of the field of lunar pyroxene composition and where it intersects with silica stability (figs. 15 (a) and (b)). Lunar pyroxenes can be more iron-rich than terrestrial ones due to lower oxygen fugacity and volatile content on the Moon, but it is not clear whether some very iron-rich pyroxenes analyzed from Apollo samples are intact or have exsolved into microscopic mixtures of olivine + silica  $\pm$  pyroxene  $\pm$  pyroxenoid (B).

Melting of lunar pyroxenes and some terrestrial pyroxenes may expose engineering equipment, such as furnaces, to free liquid silica, the presence of which may not be evident in the starting or end products. Thus, engineers should be aware of the possibility of short term or repeated interaction of furnace materials with free silica during ISRU processes.

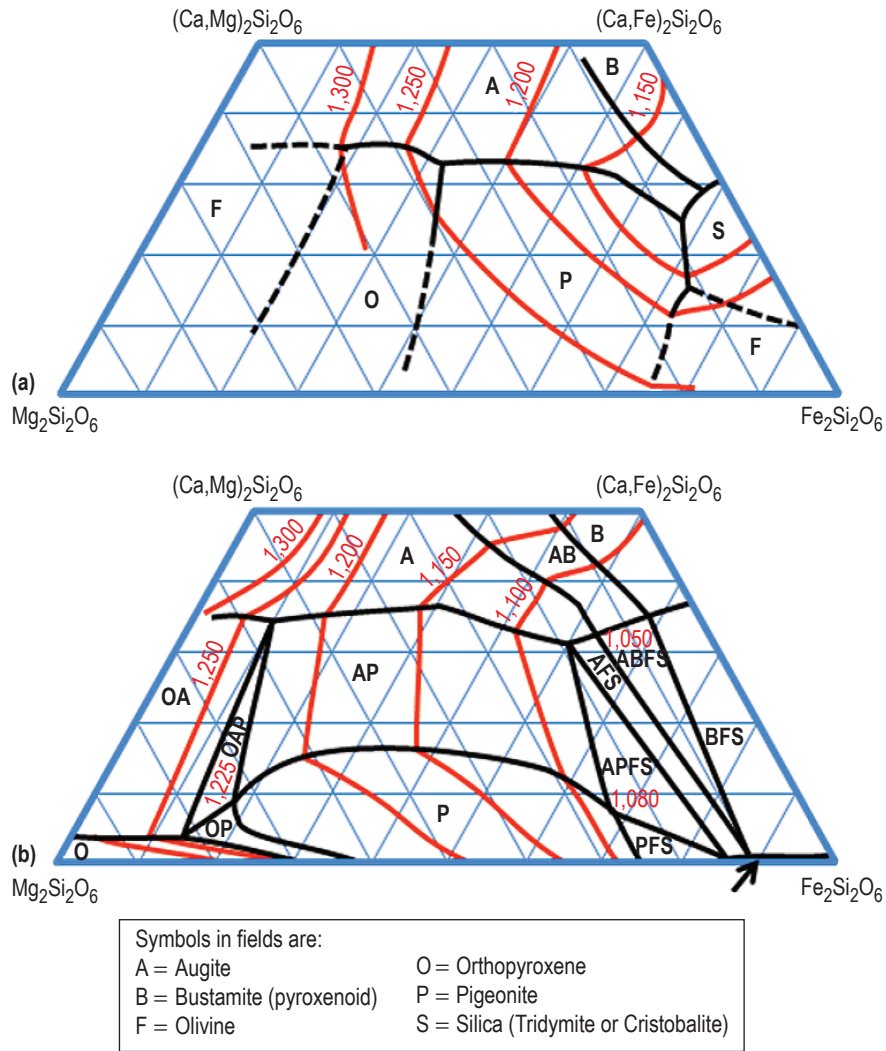


Figure 15. Pyroxene phase relations from experiments on natural terrestrial and lunar pyroxenes at 1 bar and low-oxygen fugacity. Redrawn from reference 18. Liquidus diagram (a), and solidus diagram (b).

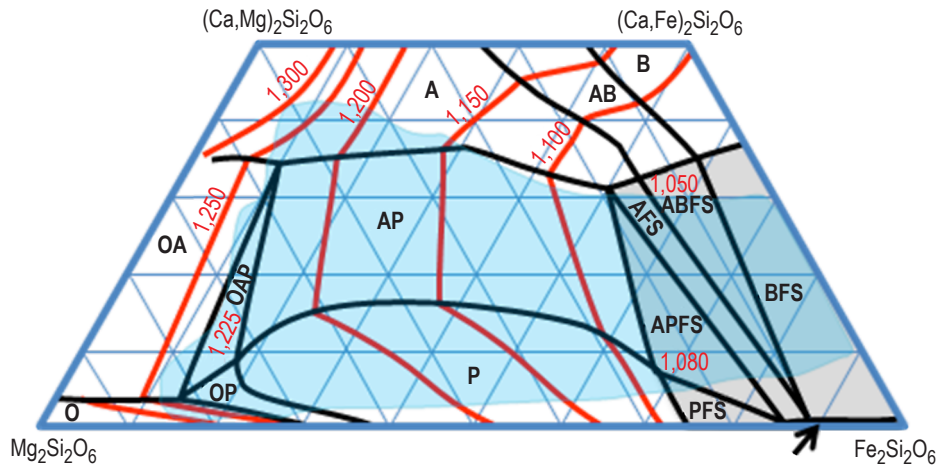


Figure 16. Solidus diagram from figure 15. The same symbols apply. The light-gray shading indicates the silica-bearing field. The blue field delineates analyzed lunar highland pyroxene compositions. The area where the two fields overlap may indicate compositions where tridymite, cristobalite, or other silicon dioxide phases may be encountered during melting.

### 3. PLAGIOCLASE

Feldspar, like pyroxene, is a name for a group of minerals. Figure 17 illustrates the compositions possible for feldspars, including compositional arrays denoting plagioclase ( $\text{Na}[\text{AlSi}_3\text{O}_8]$ - $\text{Ca}[\text{Al}_2\text{Si}_2\text{O}_8]$ ) and orthoclase ( $[\text{K},\text{Na}][\text{AlSi}_3\text{O}_8]$ ) solid solutions in gray and yellow. The vast majority of lunar feldspars are plagioclase, thus they will be the topic of the following discussion.

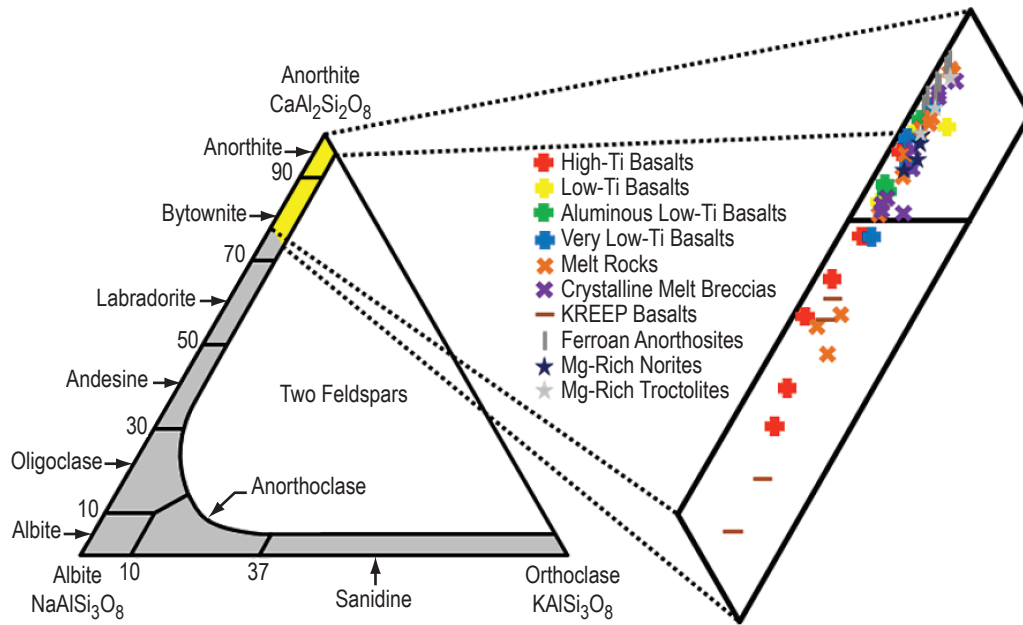


Figure 17. Feldspar ternary diagram denoting the compositional ranges of feldspars. Original diagram redrawn from reference 11. Lunar plagioclase data from reference 19.

The plagioclase field denotes feldspars that form a solid solution from anorthite (An) ( $\text{CaAl}_2\text{Si}_2\text{O}_8$ ) to albite ( $\text{NaAlSi}_3\text{O}_8$ ). The solid solution is allowed by the charge balancing effect of coupled substitution ( $\text{Na}^{+1}\text{Si}^{+4} \leftrightarrow \text{Ca}^{+2}\text{Al}^{+3}$ ). Lunar An tends to have more  $\text{Fe}^{+2}$  in its structure compared to terrestrial Ans; therefore, the lunar community often refers to lunar anorthosites as ‘ferroan anorthosites.’ Note from figure 17 that plagioclase can also contain up to 5 mole % K.<sup>11</sup>

Other trace cations in the plagioclase structure are  $\text{Mg}^{+2}$ ,  $\text{Ba}^{+2}$ ,  $\text{Sr}^{+2}$ , and  $\text{Rb}^{+1}$ . Rare-earth elements (La-Lu) may substitute for Al because they all have a +3 ionic charge. One significant rare-earth element, particularly in lunar samples, is Eu, which can have a +2 or +3 ionic charge. Since the environment on the Moon is so reducing, a large amount of Eu exists as a +2 cation. This makes it easier for Eu to substitute into the plagioclase structure relative to other rare-earth



elements. Hence, when compared to the other rare-earth elements, a large spike in Eu can be seen (called a ‘positive Eu anomaly’). This also leads to depletion in Eu in magmas that have produced plagioclase on the Moon relative to other rare-earth elements (a ‘negative Eu anomaly’).

The vast majority of terrestrial plagioclase is not An, particularly An with a minimum of sodium substitution such as lunar ferroan anorthosites (fig. 18). For example, the Stillwater plagioclase ranges from An<sub>60</sub>–An<sub>88</sub> and would thus be classified as labradorite and bytownite.<sup>20</sup> The higher-calcium plagioclase minerals in the Stillwater Complex would be more suited to reproducing the composition of some mare basalt plagioclase (fig. 19).

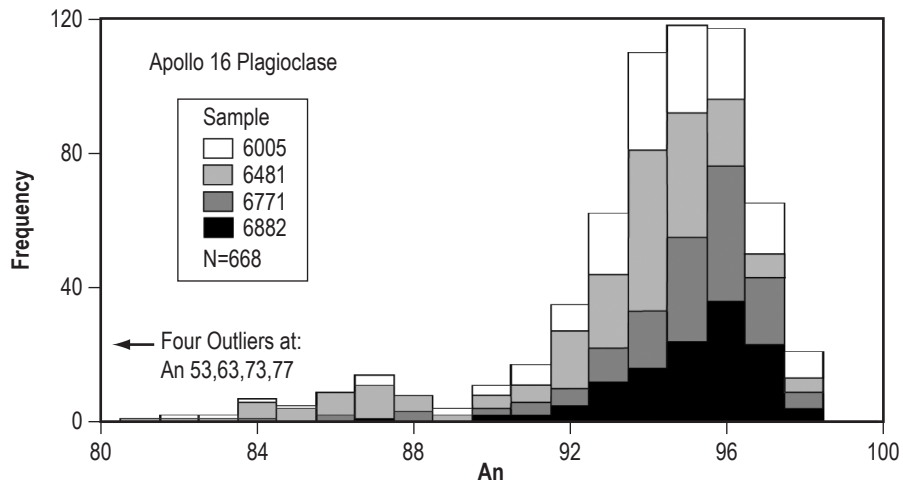


Figure 18. Plagioclase composition histogram for the Apollo 16 site, dominated by ferroan anorthosites. Note the high molar percentage of Ca in the plagioclase structure (denoted by modal percent An). Data compiled from reference 16 and other sources.

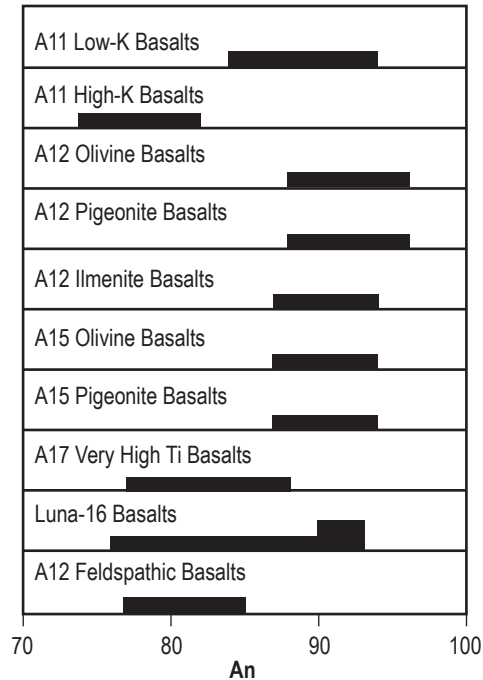


Figure 19. Plagioclase compositions in mare basalts where An indicates molar percentage of Ca in the plagioclase structure.<sup>17</sup>

### 3.1 Plagioclase Melting Phase Equilibria for In Situ Resource Utilization

ISRU may require melting of plagioclase. The crystallization temperature of a mineral (and its resulting composition) is highly dependent on the pressure of formation and the abundance of water in the melt. Figure 20 illustrates the stability fields (i.e., the possible mineral compositions) of feldspars based on the temperature and pressure of formation. Those feldspars that form as intermediate compositions will exsolve upon cooling to equilibrate with their lower temperature or pressure conditions. Figure 21 illustrates the affect of water on the temperature of formation for plagioclase compositions; however, evidence suggests anhydrous conditions for lunar crust formation.<sup>21</sup> This is not true for terrestrial plagioclase, although the crystal structure of plagioclase rarely incorporates water during formation.

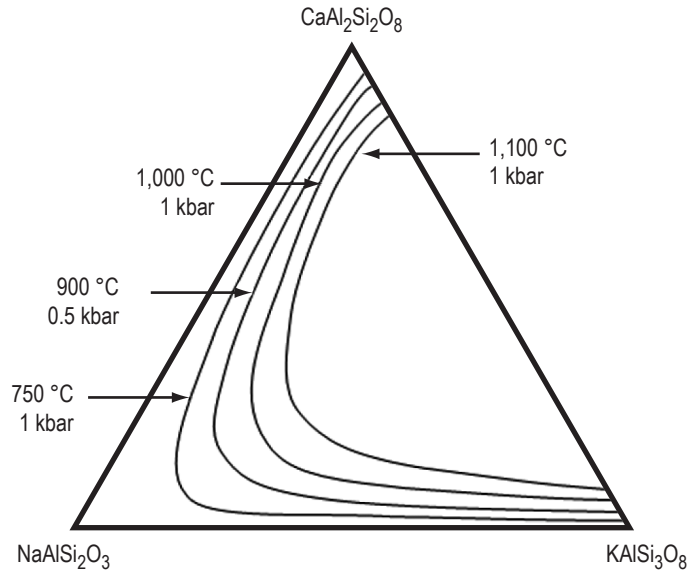


Figure 20. Feldspar ternary diagram indicating possible stable compositional ranges of feldspars with different temperatures and pressures of solidification. Diagram redrawn from reference 11 after reference 22.

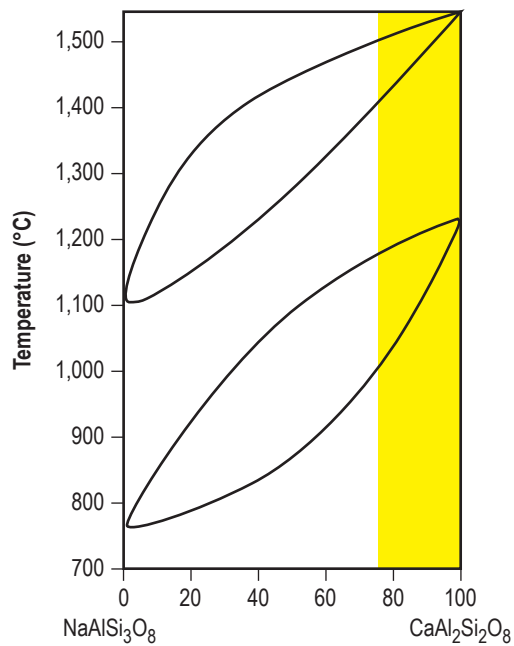


Figure 21. Plagioclase binary diagram,<sup>11</sup> indicating solidus and liquidus temperatures for anhydrous conditions (top)<sup>23</sup> and 5-kbar  $\text{H}_2\text{O}$  conditions (bottom).<sup>24</sup> The highlighted area indicates compositions of lunar plagioclase.<sup>17</sup> Note that evidence suggests anhydrous conditions for the formation of lunar rocks.<sup>21</sup>

## 4. OLIVINE

Olivine is yet another name for a group of minerals of importance to most terrestrial and lunar applications. This group includes forsterite (Fo) ( $\text{Mg}_2\text{SiO}_4$ ) and fayalite ( $\text{Fe}_2\text{SiO}_4$ ). In this solid solution, Mg and Fe substitute directly for each other as they are both +2 cations. Other +2 cations tend to substitute easily into the olivine structure, such as trace amounts of Ni and Mn. Sometimes Al,  $\text{Fe}^{+3}$ ,  $\text{Cr}^{+3}$ , and  $\text{Ti}^{+4}$  can substitute into the structure, depending on the surrounding trace elements and voids necessary to maintain charge balance in the olivine structure. Rare-earth elements can also substitute because they have a +3 ionic charge; however, heavy rare-earth elements are incorporated more often into the olivine structure as they have smaller ionic radii than the light rare-earth elements.

Figures 22 and 23 illustrate the range in compositions of lunar olivines. Note from the diagrams that lunar olivines can vary in composition nearly across the Fo-fayalite solid solution, but the average of the highlands regolith olivines is approximately 75% modal Fo ( $\text{Fo}_{75}$ ), whereas mare olivines average around  $\text{Fo}_{65}$ .

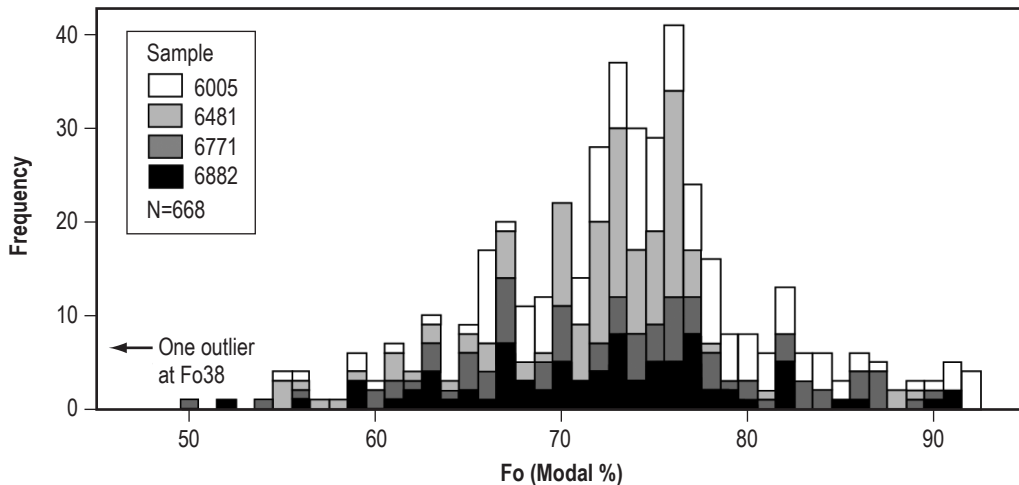


Figure 22. Olivine compositions from Apollo 16 regolith samples. Data compiled from reference 16 and other sources.

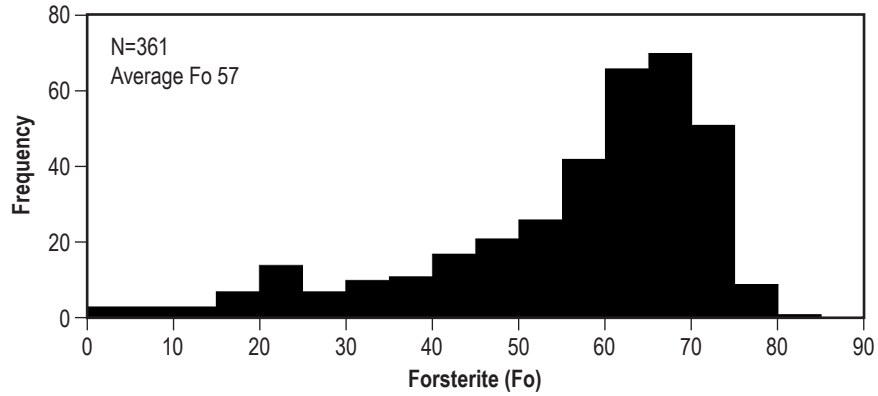


Figure 23. Mare basalt olivine compositions from Apollo missions 11, 12, 15, and 17, with data from Luna 16 and Luna 24. Data compiled from reference 25 and other sources.

#### 4.1 Olivine Melting Phase Equilibria for In Situ Resource Utilization

Like plagioclase, Fo and fayalite olivine minerals form a solid solution; therefore, a binary melting diagram is applicable to ISRU techniques. Figure 24 denotes the melting temperatures of the solid solution between Fo and fayalite.

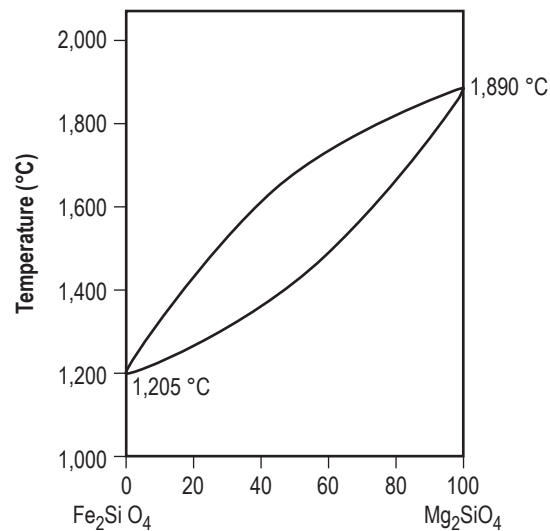


Figure 24. Solidus (bottom) and liquidus (top) temperatures for the Fo-fayalite solid solution at 1 bar pressure. Redrawn from reference 26.

## 5. REGOLITH SIMULANT NAMING PROTOCOL

### 5.1 Scope

This protocol shall be used in naming simulants produced under the direction of the NASA Marshall Space Flight Center (MSFC) Lunar Simulant Development effort.

### 5.2 Objective

The objective is to provide a uniform naming scheme that is relatively simple yet adequately robust. Names need to be succinct and useable but need to convey a significant amount of information as to the producer, the material simulated, grain size, and the version within a series. In choosing the scheme, this effort has been guided by the expertise of Dr. Steve Wilson, the U.S. Geological Survey (USGS) chemist responsible for reference materials.

### 5.3 Justification

A major consideration is the practical use of the protocol over the life of the exploration architecture as planned. Multiple generations of simulants will be made by multiple organizations. A uniform naming scheme is required to minimize confusion in the procurement and use of the simulants.

### 5.4 Protocol

The basic identifier (i.e., the name) of the simulant consists of three major parts separated by hyphens. The major parts may be divided into subparts. The general pattern is

ID-BCF-NGr,

where:

Part 1

ID    Originator ID

Examples:

NU    NASA/USGS

ORB   Orbitec

Part 2

B     Solar system body

Examples:

L Lunar  
M Martian

C General class of material being emulated.

Examples:

M Mare  
H Highland

F Fidelity

Examples:

S Simulant models as specific lunar sample/type  
T Simulant broadly models a type of geologic terrane.

There is some flexibility built into the protocol for C and F. It is expected that unforeseen developments will lead to additional classes of simulants (such as deposits or formations within terranes) and desired levels of fidelity.

### Part 3

N Production number/designator. The producer of the simulant supplies this.

Gr Grain Size designator, if appropriate (M-medium, C-coarse, D-dust, etc.) this denotes the coarsest maximum size intentionally present in the simulant. See table 1.

Table 1. Maximum\* particle size name scheme.

Design Maximum Particle Size	Term	Abbreviation
≤20 μm	Dust**	D
≤ 1 mm	Medium	M
≥4 cm	Coarse	C

\* It is assumed all size particles finer than the maximum will be present. This reflects the reality of the lunar material and the practical situation when grinding rock.

\*\* The formal definition of 'dust' by the Environmental Protection Agency and the Occupational Safety and Health Administration is ≤ 10 μm; the 20-μm design maximum particle size of the simulant reflects the difficulty of producing a simulant with a true dust maximum particle size.

An example of the basic identifier is as follows:

NU-LHT-1M,

where

NU NASA/USGS (producer)  
L Lunar (planetary body)  
H Highland  
T Type/terrane (models a broad type of materials)  
1 Series (which simulant generation), 1, 2, 3, etc.  
M Intended particle size is 1 mm or less.

### **5.5 Configuration Management**

Check the ISRU Web site at <<http://isru.msfc.gov>> for the latest version of this document.

### **5.6 Contact Information**

Contact Carole McLemore (NASA MSFC) at <[carole.a.mclmore@nasa.gov](mailto:carole.a.mclmore@nasa.gov)> for programmatic needs and Doug Rickman (NASA MSFC) at <[doug.rickman@nasa.gov](mailto:doug.rickman@nasa.gov)> for technical needs.



## 6. MINERAL SEPARATES

### 6.1 Justification

Several reasons to initially separate the constituent minerals from feedstock rocks for the production of lunar simulants are as follows:

- It permits bulk processing of rocks rather than hand processing.
- It allows use of feedstocks that would be unacceptable if used as whole rock but do contain a desired constituent.
- A broader range of constituents can be used in the simulant.
- It allows tighter constraints on reproducibility of simulants.
- It allows use of higher quality components.
- It can provide a feed to subsequent processing that has fewer contaminants.
- It permits creation of simulants with compositions outside what can be achieved by mixing whole rock.
- At large scales, it is vastly cheaper per ton than hand processing.

The existing technical approach is to mix multiple rock types, most of which are obtained from the Stillwater Complex in Montana. This is better than using a single rock but is still far short of investigators' needs, especially as it means highly skilled and senior specialists must manually select each and every piece of rock that is used. It also means investigators have to accept whatever is in the rock, alteration, undesired minerals, and all.

### 6.2 Terminology

The technology of separating minerals out of rocks is at the core of modern mining. Very few ores are pure enough to be used as extracted from the Earth; therefore, beneficiation is necessary. Beneficiation usually requires separating the minerals in a rock from each other. The general term for the study of the processes involved is extractive metallurgy.

At industrial scales, the objective of beneficiation is to isolate a desirable mineral from the source rock and to concentrate it as much as is economically practical. This desired fraction of the rock is therefore referred to as the 'concentrate' or the 'con' for short. The remaining fraction, which is waste, is referred to as the 'tails.' On small scales, it is sometimes desired to retain all or most of the minerals in the rock while isolating them from each other. In such cases, the individual 'splits' may also be referred to as 'mineral separates.'

In beneficiation of terrestrial ores, the first step is usually to crush the rock. Crushing does not liberate individual crystals within the rock from each other. This is the function of grinding. Crushing is done to provide a feed small enough to go into the grinding operation. Crushing and grinding rock, generically termed 'milling,' are very energy intensive, so leaving the material as coarse as possible is very desirable. However, the mineral being sought must be mechanically freed so it can be isolated from the undesired material (the 'gangue'). The process of freeing the target material from the gangue is termed 'liberation.' Perfect liberation is never practical or necessary. Therefore, in developing a process flow for beneficiation, the degree of liberation needed must be evaluated.

Particle size distributions are controlled throughout the crushing and grinding steps. In addition to the cost of energy, this is done because various physical and chemical processes become more and less dominant as size changes. The specific beneficiation processes used are driven by complex interactions of these parameters; therefore, controlling the size simplifies process control. Of special concern in many cases are those particles referred to as 'fines.' These are particles that are smaller than the desired size. Besides being affected differently by the processing regime, they frequently have markedly different composition compared to the bulk material being processed.

### **6.3 Evaluation Criteria**

In mining, the criteria for evaluation of beneficiation are extremely important. Excessive criteria can easily raise cost so high as to make processing economically untenable. The criteria are usually phrased based on the following:

- What is the cost of the processing?
- From the total in the feedstock, what percentage of the target material must be retained? This is termed 'recovery rate.'
- What is the desired purity of the concentrate?
- How much of the desired material can be in the tails?
- What is the amount of the tails?

These are not independent variables. They reflect differing views of the same problem because of different concerns.

Commercially, the preceding criteria are subject to rigorous engineering analysis. Such analysis is not available at this time for simulant production. Therefore, professional judgment of the project scientist, Doug Rickman, was used for criteria. For initial work, the following criteria were used:

- Target a plagioclase concentrate.
- Use 'road norite' feedstock or equivalent.
- Remove at least 50% of the pyroxenes.
- Make a concentrate with a minimum of 80% plagioclase and target of >90% plagioclase.

- The amount of waste is not relevant.
- Particles >0.5 mm are desirable.
- Determine the degree of liberation as a function of particle size

#### 6.4 Feedstock Description: Stillwater Norite

The first target of separation has been the production of a plagioclase concentrate from noritic material obtained courtesy of the Stillwater Mining Co, Nye, Montana. The Stillwater mine is working in rock known as the Stillwater Complex, which is technically referred to as a layered mafic intrusive. The plagioclase in this rock has unusually high calcium content,  $>An_{86}$ . Most terrestrial anorthosites have An values 10 to 40 points below the plagioclase in the Stillwater norites. This includes the An value of the Stillwater anorthosites. Most lunar plagioclase is  $>An_{90}$ . However, the associated pyroxenes in the Stillwater norites are not ideal for lunar simulants. Their ratio of clinopyroxene to orthopyroxene is roughly 1:6, whereas the lunar material is closer to 1:2 or higher. Also, there are hydrothermal alteration minerals in the Stillwater rocks. Thus, the Stillwater norites have good quality plagioclase but the wrong mixture of pyroxenes, and they contain undesired secondary minerals.

The following images illustrate the appearance of some of the Stillwater norite at various scales. The starting rock is a complex mixture with substantial three-dimensional variation in all properties (figs. 25 through 29).

Figure 25 is a picture of ‘road norite.’ Note the typical variation in composition (color) across the boulder. Subsequent to the production of NU-LHT-1M, the road norite has been used in many of the tests of the MSFC and USGS simulant development efforts. This was done because it was felt that this site had lower amounts of alteration minerals than the mine waste pile, which is the largest potential source of such material.

Figure 26 is a detail from figure 25. This is just below the hand sledge. The white material is plagioclase ( $\approx An_{85}$ ). The dark ‘spots’ are pyroxenes. The orthopyroxene to clinopyroxene ratio is  $\approx 3$  or  $\approx 6$  to 1. The variation in color of plagioclase and the pyroxenes is caused by a variation in the amount of hydrothermal alteration. Note the fractures in the rock. This variation is typical of this source rock.



Figure 25. Road norite. (Courtesy of USGS).



Figure 26. Detail from figure 25. (Courtesy of USGS).





Figure 27. Norite after first stage crushing. Note the wide range in color variation. This is a result of both variations in the relative abundance of pyroxenes and the amount of hydrothermal alteration. (Courtesy of USGS).

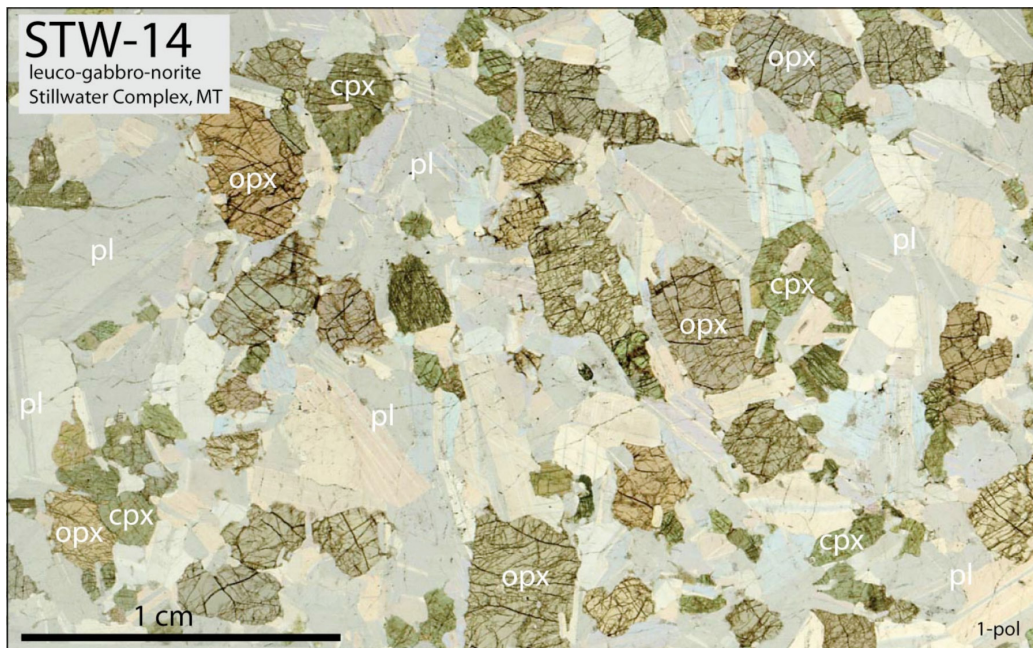


Figure 28. Thin section of Stillwater norite in plane-polarized, transmitted light. Detailed examination shows traces of alteration minerals disseminated in the pyroxenes. (Courtesy of USGS).

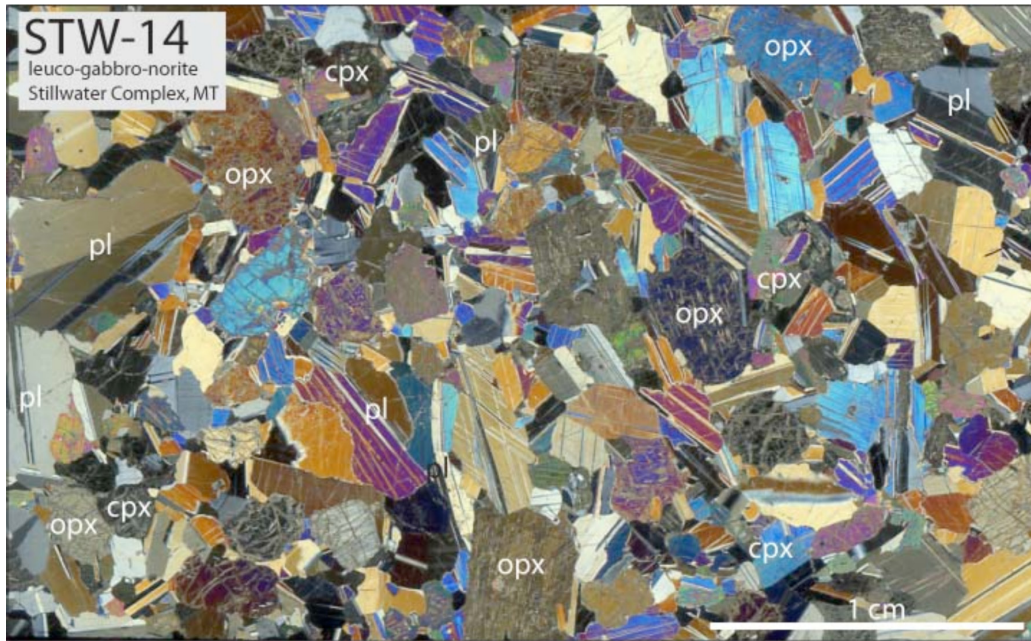


Figure 29. Same view as in figure 28 but under crossed nicols. In this thin section, the ‘smudgy’ appearance of the pyroxenes (e.g., the orthopyroxene grain in the upper left) is indicative of alteration minerals. (Courtesy of USGS).

### 6.5 Technical Results of Mineral Separation Test

The separation of the plagioclase from the pyroxenes can be done based on differences in magnetic susceptibility. The commercial company Hazen Research, Inc. established this process. Subsequently, the technical practicality of using magnetic separation of plagioclase and pyroxene from the Stillwater norite has been confirmed by work at Eriez Manufacturing Co. of Erie, Pennsylvania and at the Metallurgical and Material Engineering Department of Montana Tech of The University of Montana, Butte, Montana.

All of the minerals in the road norite are paramagnetic except the plagioclase, which is diamagnetic. Paramagnetic magnetism occurs only in the presence of an externally applied magnetic field (i.e., a paramagnetic mineral is not attracted to a magnet). Diamagnetic minerals are not magnetic even in the presence of a fairly strong magnetic field. Table 2 presents magnetic susceptibilities for the major minerals of the road norite as determined by amperage settings of a Frantz Isodynamic Magnetic Separator, Model L-1, in order of greater susceptibility.<sup>27</sup> The lower the number, the greater the magnetic susceptibility. The highest setting available on the Franz used for the study is 1.7 amps.



Table 2. Magnetic susceptibilities of the major minerals of the road norite.

Mineral	Total Range (Amps)	Best Range (Amps)
Chlorite	0.1–0.9	0.2–0.5
Hornblende	0.1–0.9	0.3–0.6
Augite	0.2–1.3	0.4–0.9
Enstatite	1–>1.7	1.3–1.5
Talc	1–>1.7	1.3–>1.7
Plagioclase (labradorite)	>1.7	>1.7

### 6.5.1 Hazen Research, Inc.

The following report on this work combines two sources. First is a report provided by Wanza Fontanelli of Hazen Research to Doug Stoeser on June 25, 2008 17:11:07–0600 in an email titled “Magnetic Separation of Pyroxene From Norite. Project 10770.” The second source is an email from Doug Stoeser to Doug Rickman on July 2, 2008 19:43 titled “Hazen separates.”

A 5.5-kg sample of the ‘road’ norite from the Stillwater Mine was provided to Hazen Research of Golden, Colorado on March 24, 2008. The objectives of this work were as follows:

1. Prepare an essentially pure feldspar product.
2. Separate the orthopyroxene, clinopyroxene, and minor iron-bearing hydrothermal alteration minerals from the plagioclase.
3. Remove hydrothermal alteration minerals.

These objectives are listed in order of significance, greatest to least, as determined during discussions with Dr. Roland Schmidt of Hazen.

Since pyroxenes, but not feldspars, are ordinarily paramagnetic, dry high-intensity magnetic separation was considered to be the best option to achieve this separation. The entire sample was initially crushed to a grain size of less than 1/4 in and a portion was screened into different size fractions for microscopic examination. This showed that good pyroxene liberation would occur at about 10 mesh. See table 3 for the conversion between mesh and microns.

Table 3. The relationship between mesh number and particle size in microns.

Mesh	Microns (µm)
10	2,000
35	500
100	149

Following this examination, the <math><1/4</math>-inch material was crushed to <math><10</math> mesh and screened at 35 and 100 mesh, making three initial splits: 10–35, 35–100, and  $\leq 100$  because magnetic separation is more selective using sized material. Each size fraction was separated with a rare-earth, high-intensity magnetic belt separator. There are several variables of the separation equipment available to the operator. Typically, these include intensity of the magnetism and the rate of feed through the system. The circuit layouts for the 10–35 split and the 35–100 split are shown in figures 30 and 31. The results of the tests are given in table 4.

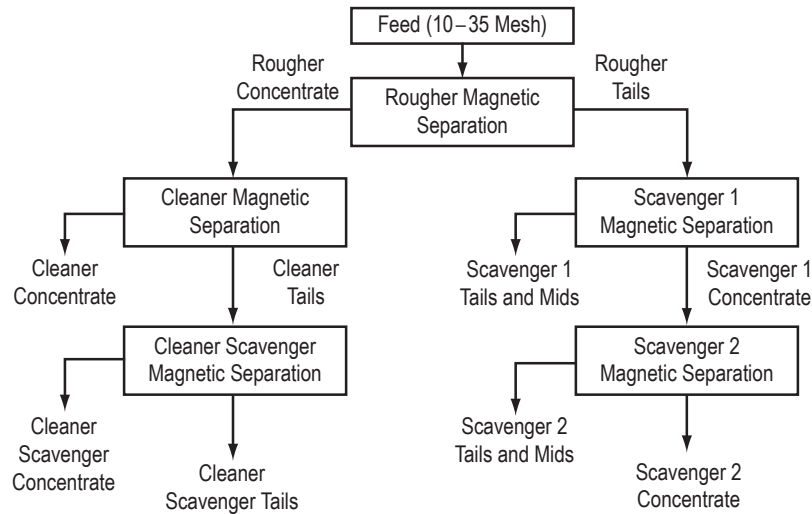


Figure 30. Flow diagram for 10–35-mesh particles from Stillwater norite by magnetic separation. Work done by Hazen Research, Inc.

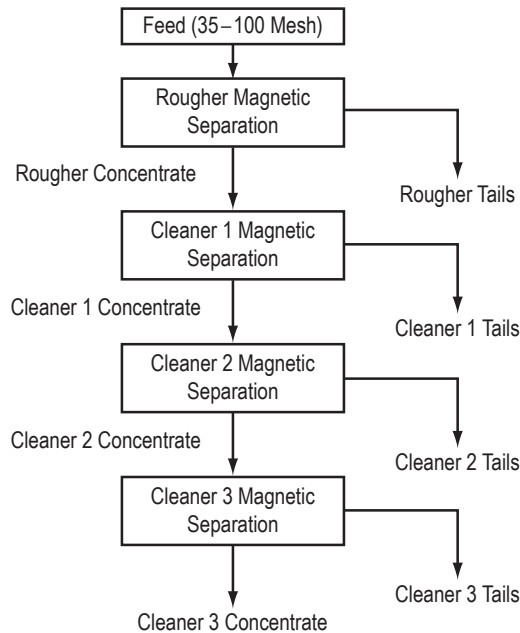


Figure 31. Flow diagram for 35–100-mesh particles from Stillwater norite by magnetic separation. Work done by Hazen Research, Inc.



Table 4. Yields of the processes in flow diagrams in figures 30 and 31.

Weight Distribution of Screen Fraction				
Product	Weight			
	(g)	(%)		
10 by 35 mesh	3,285.1	59.5		
35 by 100 mesh	1,369.7	24.8		
Minus 100 mesh	863.2	15.6		
Total	5,518	100		

Weight Distribution of Separation Products				
	Product	Weight		
		Feed to Test		Total Sample (%)
		(g)	(%)	
10 by 35 mesh	Cl-1 con	803.6	24.5	14.6
	Cl-1 scav con	69.4	2.1	1.3
	Scav-2 con	1,414.1	43	25.6
	Total con	2,287.1	69.6	41.4
	Cl-1 scav tails	63.9	1.9	1.2
	Scav-1 mids + tails	742.8	22.6	13.5
	Scav-2 mids + tails	191.3	5.8	3.5
	Total tails	998	30.4	18.1
	Total calculated feed	3,285.1	100	59.5
35 by 100 mesh	Cl-3 con	688.4	50.3	12.5
	Total con	688.4	50.3	12.5
	Ro tails	213.6	15.6	3.9
	Cl-1 tails	89.2	6.5	1.6
	Cl-2 tails	42.7	3.1	0.8
	Cl-3 tails	335.7	24.5	6.1
	Total tails	681.2	49.7	12.3
Total calculated feed	1,369.7	100	24.8	
Minus 100 mesh	Total calculated feed	863.2	100	15.6
Total feed		5,518		

Figures 32 and 33 show the concentrate (plagioclase) and the tails (dominantly pyroxenes) from the two tests described in figures 30 and 31.

Figure 32 shows the concentrate and tails from the 10–35-mesh fraction as processed according to figure 30. The concentrate is obviously cleaner (lower abundance of pyroxenes) than the source rock shown in figures 25 through 27. The plagioclase concentrate is  $\approx 95\%$  pure even at the 10–35-mesh fraction. This significantly exceeds the target purity of 90%. Thus, finer grinding is probably not necessary for this feedstock. Note the number of colors present in the tails. This indicates that the starting rocks contain multiple iron bearing minerals. Also, as the tests were to obtain a plagioclase concentrate without regard to the amount of plagioclase lost to the tails, the tails will contain some plagioclase.



Figure 32. The concentrate 32(a) and tails 32(b) from the 10–35-mesh fraction as processed according to figure 30.



Figure 33. The concentrate 33(a) and tails 33(b) from the 35–100-mesh fraction as processed according to figure 31. The photo of the tails in figure 33(b) shows marked segregation of colors

Figure 33 shows the 35–100-mesh fraction as processed according figure 31. The photo of the tails in figure 33(b) shows marked segregation of colors. This was caused simply by the method of placing the particles on the paper. A sweeping, back-and-forth hand motion was used while gently tapping the bottle. This caused the several minerals in the tails to noticeably segregate, probably due to minor differences in specific gravity of each particle.

The test separation process is significantly more complex than a single-stage separation. For example, to make the 10- to 35-mesh product, there are five separations: Rougher, cleaner, cleaner scavenger, tails scavenger 1, and tails scavenger 2. Circuit complexity is driven by costs of various inputs, product specifications, and the value of the products versus the cost of the circuit. Normally, there are three major costs incurred prior to separation processing: (1) Mining, (2) crushing, and (3) grinding. Circuit complexity typically adds little to the total cost but significantly increases product quality and recovery rates. In this case, only 936.9 g (28.5%) of the feed reported to the rougher concentrate. Of that 936.9 g, almost 7% finally reports to the tails. Of the total concentrate, 61.8% (2,287.1 g) comes from the rejected portion of the first separation. In other words, the initial, single-stage concentrate contains less than half of the total plagioclase recovered but still has significant amounts of pyroxene contamination. The full, five-stage circuit made a concentrate that is almost 70% of the feed. In contrast, the simpler processing on the finer 35–100 mesh split made a final concentrate that is only 50% of the feed.

The <100-mesh fraction, which amounts to 15.6% of the weight, was more difficult to separate. Preliminary tests with an induced roll, high-intensity, magnetic separator on a small portion indicated a good separation could be made, particularly if the very fine fraction would be removed prior to separation. Because of the relatively low weight of the <100-mesh fraction, this option was not further pursued at this time.

### **6.5.2 Hazen Research Cost Estimate**

A cost estimate was requested of Hazen Research to perform the tested process on a custom-milling basis. The amount to be processed was assumed to be individual 1-ton lots. It must be understood that custom milling in such small lots, without a guarantee of repeat business, is inherently very expensive. Furthermore, such work is not a standard part of the Hazen Research business model, though the company does do some work of this nature. Finally, the estimate was requested at a time of very high mineral prices. At such times, companies such as Hazen are generally oversubscribed and have little if any motive to minimize pricing. Therefore, the data in table 5 should be considered as illustrative and probably maximum numbers.

Table 5. Cost estimates for processing 1 ton of road norite per the flow diagrams shown in figures 30 and 31.

Task	Unit Cost (\$)	Extended Cost (\$)
<b>Sample Preparation</b> For 1 ton sample (assume 1-in top size) Stage-crush samples to minus 10 mesh Screen at 35 and 100 mesh Total cost per sample	  3,360 840 4,200	   4,200
<b>Rougher magnetic separation</b> 10-×35-mesh sample (≈ 1,200 lb) 35-×100-mesh sample (≈ 500 lb) Technical assistance Total cost per sample	 5,600 2,450 200 8,250	   8,250
<b>Cleaner and scavenger magnetic separation</b> 10-×35-mesh sample 35-×100-mesh sample Technical assistance Total cost per sample	 5,600 2,450 300 8,350	   8,350
<b>Cleanup/packaging/consumables</b> Total cost per sample	 560	 560
<b>Data compilation/report</b> Total cost	 2,000	 2,000
<b>Contingency (10%)</b>	2,340	2,340
<b>Grand total cost per sample</b>	-	25,700

## 6.6 Eriez Manufacturing Co.

Subsequently, the technical practicality of using magnetic separation of plagioclase and pyroxene from the Stillwater norite has been confirmed by work at the Eriez Manufacturing Co. of Erie, Pennsylvania and at the Metallurgical and Material Engineering Department of Montana Tech of The University of Montana, Butte, Montana. The tests at Eriez were primarily to determine how well the two pyroxenes of the road norite (enstatite and augite) could be separated.

The following is taken from email communications from Doug Stoesser to Doug Rickman, Eriez,<sup>28</sup> and Stoesser.<sup>29</sup>

Approximately 18 kg of the Stillwater road norite was sent to Eriez Manufacturing Company, Erie, PA. Eriez is a leading manufacturer of magnetic separation equipment <<http://en-us.eriez.com/>>. Eriez returned a report and the resulting splits on August 4, 2009.

### 6.6.1 Eriez methods

Eriez employed a drum and a roll rare-earth magnetic separator, Eriez model SP3RE and model RE Roll 65-1. Processing was done dry at ambient temperature and the feed material was nominally <1 mm. The basic principles of the belt-driven, rare-earth magnetic separator process are shown in figure 34. The head pulley or roller is an adjustable rare-earth magnet. Belt speed is

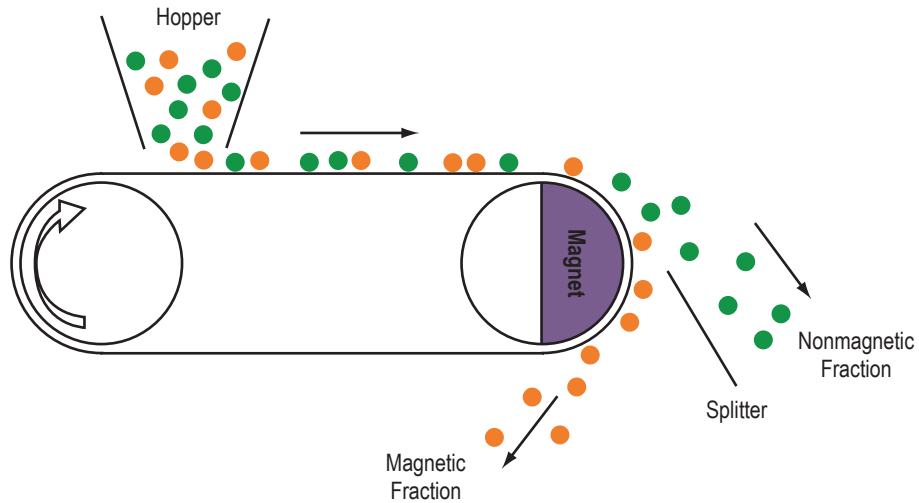


Figure 34. The basic theory of operation of a belt-driven, rare-earth, magnetic separator.

also adjustable. More magnetic material will be held longer by the drum roller and drop further back than the less magnetic material. Typically, there is a vertical partition or splitter below the roller so that the two separates (fractions) are physically isolated from each other and can be collected. More than one splitter can also be used.

Eriez found that fines were interfering with separation because of a high concentration of magnetic minerals in the fines. It should be noted that at this time the nature of the fine-grained magnetics in the road norite has not been determined. Based on geology, the minerals chromite, magnetite, and pyrrhotite are all likely candidates. To remove most of the magnetic fines, a first-stage magnetic separation was done and the magnetic fraction was dedusted to remove most of the <150-mesh fines using a Kice air classifier. A measured 8.79 wt. % of the sample went into this fraction. Subsequently, a three-stage separation was done (fig. 35). Finer and more magnetic pyroxenes were removed using a 350-fpm belt speed. Coarser and less magnetic pyroxenes were removed using a 200-fpm belt speed. The plagioclase and other nonmagnetic minerals from the first pass plus the tails of the third pass were scavenged using a 160-fpm belt speed. The nonmagnetic fraction of this step is called split 5. This process flow removed essentially all of the >150 mesh pyroxenes from the plagioclase feldspar.

The magnetic fractions other than the fines were combined and fed to the SP3RE drum. Using a drum speed of 180 fpm and a splitter setting 2 inches in front of the drum, a less magnetic concentrate was made and called split 6. The drum speed was increased to 220 fpm and the sample was split into two further fractions, about 6.4% of the most magnetic (called split 7) and 32.8% of an intermediate magnetic material (called split 8). This test is shown in figure 36.



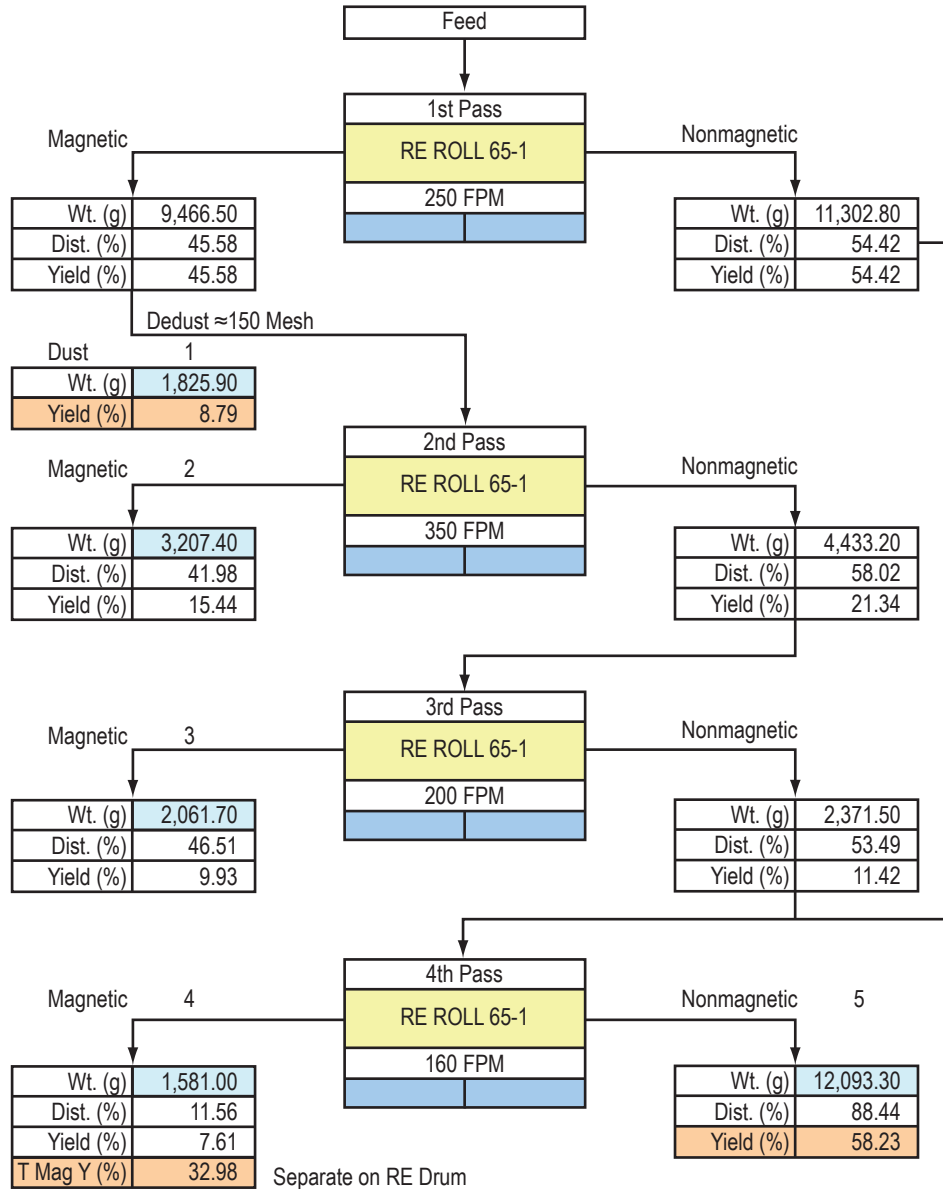


Figure 35. First pass process flow used by Eriez. Compare with figures 31 and 32. The differences reflect the different processing objectives of the work at Hazen and the work at Eriez.

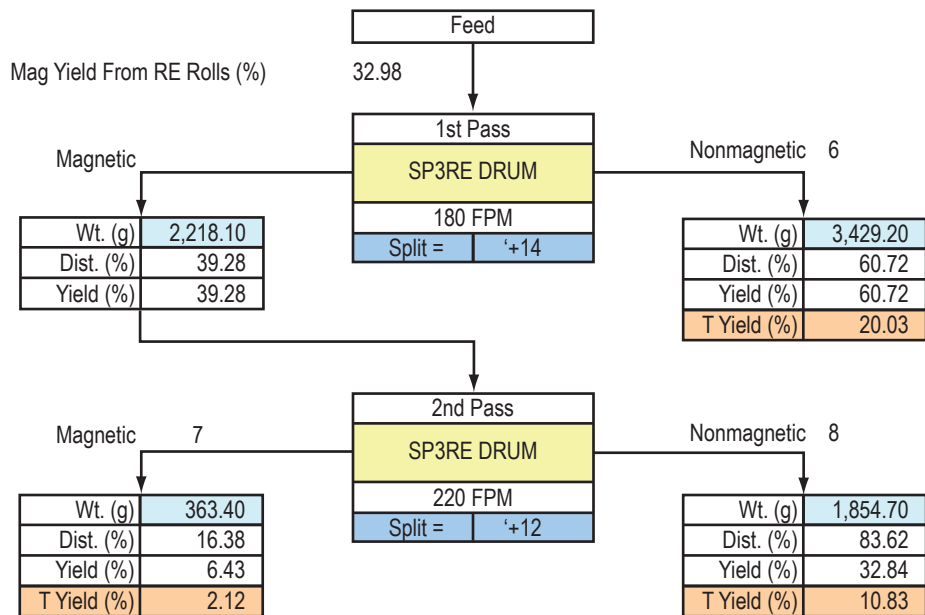


Figure 36. Second pass process flow used by Eriez. Because the feedstock for this process came from the magnetic fraction obtained from the preceding process, even splits 6 and 8 are distinctly magnetic compared to plagioclase.

Eriez suggests the preceding two process flows could be condensed into one (see fig. 37). It is worth noting that the differences between the flow sheets worked out by Hazen (figs. 30 and 31) and Eriez (figs. 35 and 36) reflect the different objectives of each. Hazen was demonstrating the production of a plagioclase concentrate. Eriez was attempting to split the clinopyroxenes and orthopyroxenes from each other.

### 6.6.2 X-Ray Diffraction Methods

Based on visual inspection, Eriez reported that ‘a clear enstatite-augite split was not seen.’ The USGS then did X-ray diffraction (XRD) analysis of the Eriez splits to determine the mineralogy of the splits and to evaluate the outcome of the Eriez work.

A 2-g aliquot of each split was transferred to a McCrone micronizing mill together with 10 mm of distilled water and milled for 4 min. The suspension was transferred to a cup and allowed to air dry. The sediment was transferred to a mortar and pestle and lightly ground to break up aggregates. The loose powder was passed through a 60-mesh sieve and then backpacked into a PANalytical sample holder for analysis. Pertinent characteristics of the XRD unit are given in table 6.

Identification of mineral phases was done with Material Data Inc. (MDI) Jade (V 9.1) search-match software using the International Centre for Diffraction Data’s ‘2009 PDF-4’ and National Institute of Standards and Technology (NIST) ‘Fachinformationszentrum Karlsruhe/ NIST Inorganic Crystal Structure Database.’

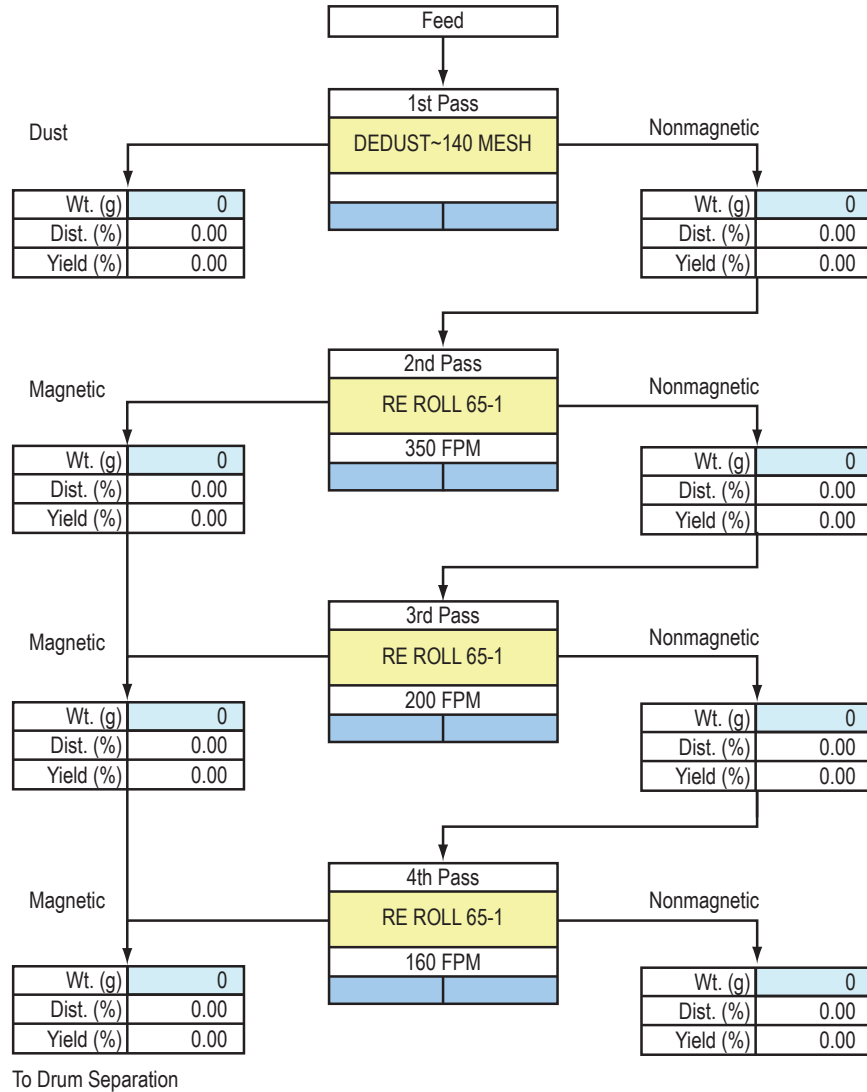


Figure 37. A conceptual rearrangement of the preceding processing flow diagrams suggested by Eriez.

Table 6. XRD instrument description used for analysis of mineral separates.

XRD Instrument	Attribute
PANalytical X'Pert Pro-MPD X-ray Diffractometer	15-mm beam mask 1/2° antiscatter slit 1/4° divergence slit 1/2° receiving antiscatter slit 1/4° receiving divergence slit Scan range of 5 to 65 degrees two-theta Theta/Theta geometry Cu long-fine-focus X-ray tube (Ni filtered) X'celerator solid state strip detector Instrument conditions are 45 kV, 40 mA Step size 0.0167° in continuous scan mode Sample spinner on scan rate was 1° per min for a total scan time of 1 hr



Semi-quantitative mineral estimates were calculated using MDI Whole Pattern Fit (WPF) software, which simultaneously calculates a WPF and a Rietveld refinement of the minerals. Reference minerals, termed ‘cards’ are selected from the integral database. The majority of the cards are ‘structure’ references that represent perfect crystals of the mineral. Each card contains a full crystallographic description of the mineral. A calculated model of the observed pattern is produced by nonlinear, least-squares optimization. The calculations, performed by the software involve the application of various parameters to improve the fit of the model to the observed data. Modeling parameters include background reduction, profile fitting, and lattice constants. Iterations minimize a residual error between the calculated XRD pattern from the selected references in comparison to the measured scan of the sample. All data were normalized to 100% based on the identified minerals.

Limitations of the XRD data are as follows:

- XRD analysis measures the crystalline portion of the sample. This does not include any amorphous phase that may be present or any organic components.
- Talc and chlorite are not easily modeled by WPF and they have a higher error associated with quantification. For these two minerals, the error is approximately plus or minus 50% of the amount reported.
- The WPF software normalizes the data to 100% for all identified phases. The typical detection limit by XRD is between 1 and 3 wt. %, depending on the crystallinity of the phase and interference from overlapping lines from other phases. Thus, there may be trace phases present but not identified, and they are not included in the model.

### 6.6.3 Results

The results of the XRD analysis are presented in table 7. Split numbers are from figures 35 and 36. The plagioclase concentrate substantially exceeds requirements, with a purity of approximately 99%. This confirms the visual analysis of the previous trial by Hazen Research Inc. Therefore, it seems probable that high-quality separation between plagioclase and pyroxene, assuming feedstock similar to the road norite, is not technically difficult.

Fitted minerals are as follows:

- Plagioclase ((Ca<sub>0.86</sub>Na<sub>0.14</sub>)(Al<sub>1.86</sub>Si<sub>0.14</sub>)Si<sub>2</sub>O<sub>8</sub>).
- Orthoenstatite (Mg(Ca<sub>0.054</sub>Mg<sub>0.946</sub>)(Si<sub>2</sub>O<sub>6</sub>)).
- Augite (diopside) (CaMgSi<sub>2</sub>O<sub>6</sub>).
- Hornblende (Na<sub>0.9</sub>K<sub>0.4</sub>Ca<sub>1.6</sub>Mg<sub>2.8</sub>Fe<sub>1.4</sub>Ti<sub>0.5</sub>Al<sub>1.4</sub>(AlSi<sub>6</sub>O<sub>23</sub>(OH))).
- Clinocllore IIb (Mg<sub>4.54</sub>Al<sub>0.97</sub>Fe<sub>0.46</sub>Mn<sub>0.03</sub>(Si<sub>2.85</sub>Al<sub>1.15</sub>O<sub>10</sub>)(OH)<sub>8</sub>).
- Talc 2M (Mg<sub>3</sub>(OH)<sub>2</sub>(Si<sub>4</sub>O<sub>10</sub>)).

The separation of the pyroxenes was not achieved in this test, but modest separation of the talc and hornblende was achieved. These are either late stage primary minerals or secondary minerals. No separation was achieved for chlorite. This is not surprising as the thin sections, figures 28 and 29, show this alteration mineral is within the pyroxene grains. Talc, hornblende, and chlorite are not desirable minerals in a lunar simulant.

Table 7. Modal mineralogy of selected splits from magnetic separations by Eriez.

Split Number	Mafic Fraction				Total Mafic Fraction (6+7+8)	Whole Sample Mineral Mode (Wt. %)
	5	6	7	8		
Mineral	Nonmag 1st Stage	Less-mag 1st Pass 2nd Stage	Mag 2nd Pass 2nd Stage	Less-mag 2nd Pass 2nd Stage		
Wt. % of whole rock	68.2	19.3	2	10.5	31.8	100
Opx (enstatite)	n.d.	55.4	51.1	63.6	57.8	18.4
Cpx (augite)	n.d.	9.6	8.2	6.4	8.4	2.7
Opx/(opx+cpx)	–	0.85	0.86	0.91	87.3	87.3
Chlorite (clinocllore)	0.6	2	2.5	3	2.4	1.2
Talc	n.d.	7	9.8	4.1	6.1	1.9
Hornblende	n.d.	3.5	3.5	0.8	2.6	0.8
Wt. % of mafic fraction	–	60.7	6.4	32.9	–	–
Plag	99.4	22.4	24.9	22.8	22.7	75

To doublecheck the XRD results, the data were used to estimate a complete modal analysis for the mafic fraction and bulk road norite. The weight percent modal plagioclase matches that estimated from a weight percent Cross, Iddings, Pirsson, and Washington (CIPW) normative analysis, thus cross-validating the respective results. The road norite is 75% plagioclase and 25% other minerals. The total rock contains 22% total pyroxene with an opx/(opx+cpx) ratio of 87%. Total weight percent of late stage minerals is 3.8% (hornblende, talc, and chlorite).

There is substantial plagioclase in the mafic splits. This is not surprising as the design was to retain all possible pyroxene in a fraction. Of necessity, this means that a high purity plagioclase fraction was produced and that some plagioclase would go with the pyroxenes. The latter is caused by an incomplete liberation of the plagioclase. Thus, there were a significant number of particles containing both plagioclase and pyroxene. Given the amount of plagioclase in the mafic splits, if there is a preferential locking of the plagioclase to one or the other pyroxene, it could certainly affect the assessment of separation efficiency between the pyroxenes. There are no data at this time to evaluate this possibility. In figure 28, there are more small grains of plagioclase within the clinopyroxene than in the orthopyroxene, but this sample is far too limited to suggest an answer.

## 6.7 Analysis

The values for the magnetic susceptibility of enstatite versus augite pyroxene (table 2) suggest they can be separated by a magnetic technique. The values shown also suggest that augite cannot be easily separated from chlorite and hornblende if those minerals are also present. The same is true for enstatite and talc. The ranges of susceptibility for the two pyroxenes suggest that actual susceptibility values should be determined for the specific pyroxenes present in the target material, in this case the road norite. In any case, mineral separation is always custom work that requires trial runs on the specific equipment used.

It should be noted that two pyroxenes in a gabbroic rock are not typically present as separate grains of each mineral. In plutonic gabbroic rocks, the pyroxenes first form as a high-temperature phase and, as they cool, invert to the low-temperature form. When this occurs, exsolution lamellae on the scale of a few to tens of microns form in the crystals (clinopyroxene lamellae in

the orthopyroxene and vice versa). Where this occurs, complete liberation of the two pyroxenes requires grinding to a grain size of around 5  $\mu\text{m}$  or less. Otherwise pure separates cannot be achieved.

Not only did this study provide an independent estimate of the modal amount of plagioclase in the road norite at 75 wt. %, it also provided an estimate of the proportion of pyroxene. It was clear in hand samples of the road norite that orthopyroxene greatly outnumbered clinopyroxene, and the measured percentage of orthopyroxene to total pyroxene of 87% is quite reasonable based on hand sample analysis. Note that the XRD results (fig. 26) indicate an average  $\text{An}_{86}$  composition, which matches well with the previously calculated  $\text{An}_{87}$  value from bulk chemistry of the road norite.

Information on the types of minor and alteration minerals present is an added bonus of the XRD work. The occurrence of chlorite and talc in the sample is not a surprise but the hornblende was. Hornblende could form as a high-temperature intercumulus phase if some water was present late in the crystallization of the road norite. It could also be a high temperature metamorphic phase. Without petrographic analysis, its source is unknown. The genetic source can be significant, as it can strongly affect how easy it is to remove the mineral. Talc is not an alteration product of pyroxene and it may have been introduced from the nearby ultramafic zone.

The fact that the <150-mesh fines were distinctly more magnetic than the bulk rock is also noteworthy. To date, no mineralogical analysis has been done of this fraction.

## 6.8 Bushveld

The Bushveld Complex of South Africa, like the Stillwater Complex, is a layered mafic intrusion. Some of the rock from this source is sold as dimension stone in the U.S. under various trade names. 'Impala Black' (figs. 38 and 39) is a common variant. It is also referred to as 'Nero Impala,' 'Rustenburg Granite,' and 'Rustenburg Gabbro.'

The Impala Black is very attractive as a potential source of pyroxene material for lunar simulants. First, the rock has very low amounts of alteration minerals. Second, the clinopyroxene to orthopyroxene ratio varies substantially in a highly consistent and reproducible manner. In principle, it is possible to find almost any desired clinopyroxene to orthopyroxene ratio within the Bushveld Complex. Third, the known reserves of the material are enormous, meaning it will be available for a long time and in large amounts. One producer of Impala Black produces approximately 50,000  $\text{m}^3$  of stone a year. This is approximately 10% of the rock moved, as most of the rock moved is waste (Jonathan Houghton, pers. comm., June 3, 2010). Much of the waste would be highly suitable for the purpose of simulant production.

However the plagioclase in the Bushveld rocks has a much lower An value than the Stillwater rock. Therefore, separation of the plagioclase from the pyroxenes would be necessary. Having demonstrated the technical feasibility of such separation using the Stillwater rock, which is very similar to the Impala Black, this does not seem to be a technical problem. Cost is a concern. In addition to the cost of the crushing and separation, there is also a cost of shipping. Estimates of shipping costs from South Africa to the U.S. on a per-ton basis vary from a few hundred dollars to \$16,500.



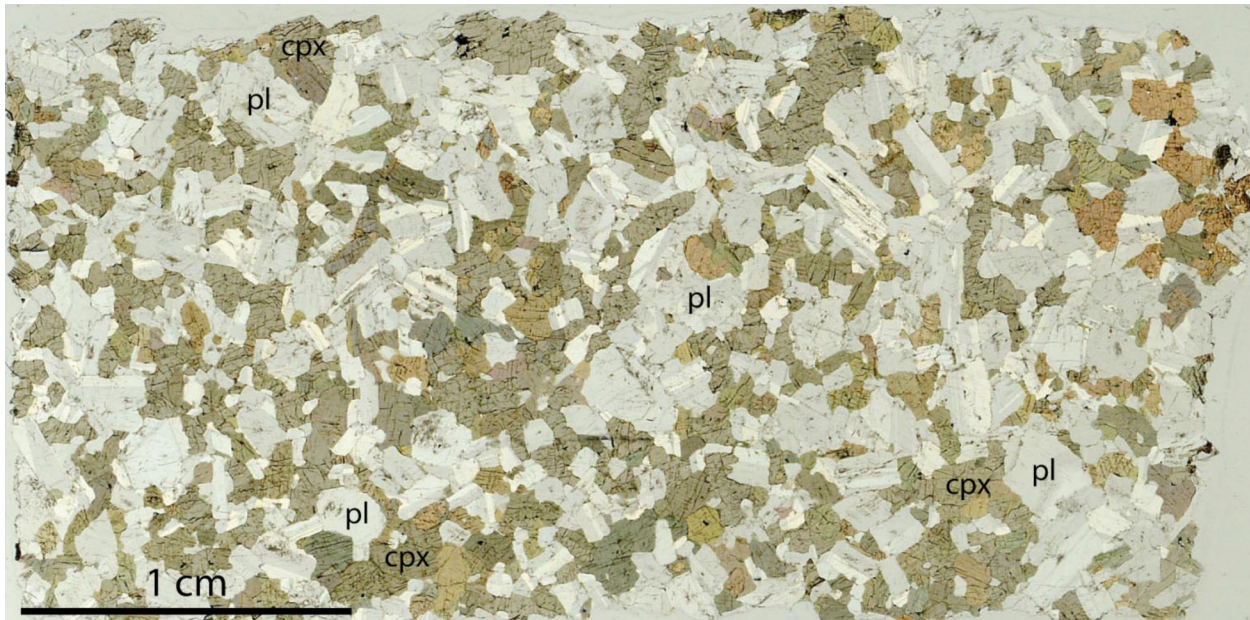


Figure 38. Impala Black in plane-polarized, transmitted light (clinopyroxene and plagioclase). (Courtesy of USGS).

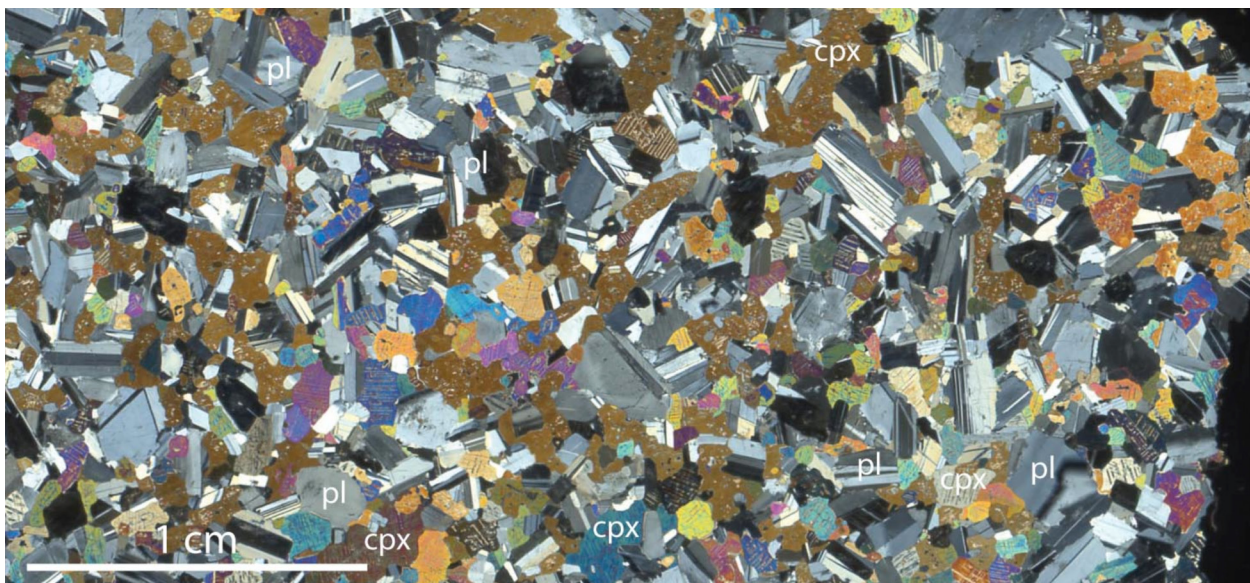


Figure 39. Same view as in figure 38 but under crossed nicols. Compare with figures 28 and 29. (Courtesy of USGS).

When estimating the magnitude of rock that would need to be shipped, it must be remembered that the amount of pyroxene needed varies substantially. In many scenarios, relatively small amounts are needed to achieve target compositions. Both the targeted lunar composition and the

composition of the other terrestrial sources used will have an effect. For example, if the target composition has 25% total pyroxenes with a clinopyroxene to orthopyroxene ratio of 0.5 and the other feedstock is Stillwater road norite, then only  $\approx 100$  kg of a pure clinopyroxene concentrate would be needed.

Figures 40 and 41 illustrate the magnitude and quality of the resource potentially available. The images are taken from Jonathan Houghton with permission.<sup>30</sup>



Figure 40. A quarry that produces the dimension stone Impala Black. This is but one of many quarries operated by M+Q and producing this specific stone. Image by Jonathan Houghton.





Figure 41. Working faces in quarry shown in figure 40. Almost all of the rock in view is functionally identical for the purposes of simulant utility. Image by Jonathan Houghton.

## REFERENCES

1. Le Maitre, R.W.: *Igneous Rocks: A Classification and Glossary of Terms: Recommendations of the International Union of Geological Sciences, Subcommittee on the Systematics of Igneous Rocks*, Cambridge University Press, 236 pp, 2002.
2. Ashwal, L.D.: *Anorthosites*, Springer-Verlag, Berlin, Germany, 422 pp, 1993.
3. Wilhelms, D.E.; McCauley J.F.; and Trask N.J.: “The Geologic History of the Moon,” *USGS Professional Paper*, 1348 pp, 1987.
4. Stöffler, D.; Knoell H.-D.; Marvin U. B.; et al.: *Recommended Classification and Nomenclature of Lunar Highland Rocks—A Committee Report*, In Conference on the Lunar Highlands Crust, November 14-16, 1979, Houston, TX, Pergamon Press, pp. 51—70, 1980.
5. Le Bas, M.J.: “Report of the Working Party on the Classification of the Lunar Igneous Rocks,” *Meteoritics and Planetary Sci.*, Vol. 36, pp. 1183–1188, 2001.
6. Stöffler, D.; and Grieve, R.A.F.: “Impactites. Recommendations by the IUGS Subcommittee on the Systematics of Metamorphic Rocks,” *IUGS Subcommittee on the Systematics of Metamorphic Rocks*, Vol. 15, 2007.
7. Reimold, W.U.; Horton, J.W.; and Schmitt, R.T.: *Debate About Impactite Nomenclature—Recent Problems*, In Large Meteorite Impacts and Planetary Evolution IV, Vredefort Dome, South Africa, Abstract # 3033, August 17–21, 2008.
8. Vaniman, D.T.; and Papike, J.J.: “The Lunar Highland Melt-Rock Suite,” *Geophys. Res. Let.*, Vol. 5, pp. 429–432, 1978.
9. Stöffler, D.; Knoll, H.-D.; and Maerz, U.: Terrestrial and Lunar Impact Breccias and the Classification of Lunar Rocks,” *Proceedings of the 10th Lunar and Planetary Science Conference*, pp. 639–675, 1979.
10. Ryder, G.: Distribution of Rocks at the Apollo 16 Landing Site,” O.B. James and F. Hörz (eds.), *LPI Technical Report 81-01*, In Workshop on Apollo 16, Lunar and Planetary Institute, pp. 112–119, 1981.
11. Deer, W.A.; Howie, R.A.; and Zussman, J.: *An Introduction to the Rock-Forming Minerals*, 2nd Edition, Longman Scientific and Technical, Harlow, Essex, England. 696 pp., 1992.
12. Papike, J.J.; Ryder, G.; and Shearer, C.K.: “Lunar Samples in Planetary Materials,” J.J. Papike (ed.), Mineralogical Society of America, *Rev. in Miner.*, Vol. 36, , pp. 5–01 to 5–189, 1998.

13. Morimoto, N.: "Nomenclature of Pyroxenes," *Mineralogical Mag.*, Vol. 52, pp. 535–550, 1988.
14. Heiken, G.; Vaniman, D.; and French, B.M.: *Lunar Sourcebook: A User's Guide to the Moon*, Cambridge University Press, Cambridge [England], New York, NY, 736 pp., 1991.
15. Gaines, R.V.; Skinner, H.C.W.; Foord, E.E.; et al.: *Dana's New Mineralogy*, John Wiley & Sons, Inc., New York, NY, 1819 pp., 1997.
16. Simkin, T.; Noonan, A.F.; Switzer, G.S.; et al.: "Composition of Apollo 16 Fines 60051, 60052, 64811, 64812, 67711, 67712, 68821, and 68822," *Proceedings of the 4th Lunar Science Conference, Geochimica et Cosmochimica, Acta.* 1, Sup. 4, pp. 279–290, 1973.
17. Papike, J.J.; Hodges, F.N.; Bence, A.E.; et al.: "Mare basalts: Crystal chemistry, Mineralogy, and Petrology," *Rev. in Geophys. and Space Phys.*, Vol. 14, pp. 475–540, 1976.
18. Huebner, J.S.; and Turnock, A.C.: "The Melting Relations at 1 Bar of Pyroxenes Composed Largely of Ca-, Mg-, and Fe-Bearing Components," *Amer. Miner.*, Vol. 65, pp. 225–271, 1980.
19. Papike, J.; Taylor, L.; and Simon S.: *Lunar Minerals in Lunar Sourcebook: A User's Guide to the Moon*, G.H. Heiken, D.T. Vaniman, and B.M. French (eds.), Cambridge University Press, Cambridge, United Kingdom, pp. 121–182, 1991.
20. McCallum, I.S.: *The Stillwater Complex in Layered Intrusions*, R.G. Cawthorn (ed.), Developments in Petrology 15, Elsevier Scientific Publishing Company, Amsterdam, Netherlands, pp. 441–483, 1996.
21. Sharp, Z.D.; Shearer, C.K.; McKeegan, K.D.; et al.: "The Chlorine Isotope Composition of the Moon and Implications for an Anhydrous Mantle," *Sci.*, doi: 10.1126/science.1192606, 2010.
22. Fuhrman, M.L.; and Lindsley, D.H.: "Ternary-Feldspar Modeling and Thermometry," *Amer. Mineral.*, Vol. 73, pp. 201–215, 1988.
23. Bowen, N.L.: "Melting Phenomena in Plagioclase Feldspars," *Amer. J. of Sci.*, Vol. 35, pp. 577–599, 1913.
24. Yoder, H.S.; Stewart, D.B.; and Smith, J.R.: "Ternary Feldspars," *Carnegie Institution of Washington Yearbook*, Vol. 56, pp. 206–216, 1957.
25. Meyer, C.: "Lunar Sample Compendium," <<http://curator.jsc.nasa.gov/lunar/compendium.cfm>>, accessed 2008.
26. Klein, C.; and Hurlbut, C.S., Jr.: *Manual of Mineralogy*, 21st edition, John Wiley and Sons, Inc., New York, NY, 1993.



27. Rosenblum, S.; and Brownfield, I.K.: "Magnetic Susceptibilities of Minerals: U.S. Geological Survey Open-File Report," *OFR 99-0529*, 11p., <<http://pubs.usgs.gov/of/1999/ofr-99-0529/>>, accessed 1999.
28. *Eriez Magnetic Research and Development Test Summary: Separation of Stillwater Norite Minerals*, Eriez Manufacturing Company, Erie, PA, July 31, 2009.
29. Stoesser, D.B.: "XRD Results for Eriez Magnetic Separates of the Stillwater Road Norite," *NASA USGS Simulant Development and Characterization Project Internal Project Report*, Nov 30, 2009.
30. Houghton, J.: *NASA Nero Impala Quarries, South Africa, M+Q North American, Dacula, GA*, unpublished, 2010.

REPORT DOCUMENTATION PAGE			Form Approved OMB No. 0704-0188		
<p>The public reporting burden for this collection of information is estimated to average 1 hour per response, including the time for reviewing instructions, searching existing data sources, gathering and maintaining the data needed, and completing and reviewing the collection of information. Send comments regarding this burden estimate or any other aspect of this collection of information, including suggestions for reducing this burden, to Department of Defense, Washington Headquarters Services, Directorate for Information Operation and Reports (0704-0188), 1215 Jefferson Davis Highway, Suite 1204, Arlington, VA 22202-4302. Respondents should be aware that notwithstanding any other provision of law, no person shall be subject to any penalty for failing to comply with a collection of information if it does not display a currently valid OMB control number.</p> <p><b>PLEASE DO NOT RETURN YOUR FORM TO THE ABOVE ADDRESS.</b></p>					
1. REPORT DATE (DD-MM-YYYY) 01-01-2011		2. REPORT TYPE Technical Memorandum		3. DATES COVERED (From - To)	
4. TITLE AND SUBTITLE  Notes on Lithology, Mineralogy, and Production for Lunar Simulants			5a. CONTRACT NUMBER		
			5b. GRANT NUMBER		
			5c. PROGRAM ELEMENT NUMBER		
6. AUTHOR(S)  D.L. Rickman, D.B. Stoeser,* W.M. Benzel,* C.M. Schrader,** and J.E. Edmunson***			5d. PROJECT NUMBER		
			5e. TASK NUMBER		
			5f. WORK UNIT NUMBER		
7. PERFORMING ORGANIZATION NAME(S) AND ADDRESS(ES) George C. Marshall Space Flight Center Marshall Space Flight Center, AL 35812			8. PERFORMING ORGANIZATION REPORT NUMBER  M-1303		
9. SPONSORING/MONITORING AGENCY NAME(S) AND ADDRESS(ES) National Aeronautics and Space Administration Washington, DC 20546-0001			10. SPONSORING/MONITOR'S ACRONYM(S) NASA		
			11. SPONSORING/MONITORING REPORT NUMBER NASA/TM-2011-216454		
12. DISTRIBUTION/AVAILABILITY STATEMENT Unclassified-Unlimited Subject Category 91 Availability: NASA CASI (443-757-5802)					
13. SUPPLEMENTARY NOTES Prepared by the Earth Sciences Office * United States Geological Survey Denver Federal Center, Denver, CO, ** Oak Ridge Associated Universities, Oak Ridge, TN, *** BAE Systems, Huntsville, AL					
14. ABSTRACT The creation of lunar simulants requires a very broad range of specialized knowledge and information. This document covers several topic areas relevant to lithology, mineralogy, and processing of feedstock materials that are necessary components of the NASA lunar simulant effort. The naming schemes used for both terrestrial and lunar igneous rocks are discussed. The conflict between the International Union of Geological Sciences standard and lunar geology is noted. The rock types known as impactites are introduced. The discussion of lithology is followed by a brief synopsis of pyroxene, plagioclase, and olivine, which are the major mineral constituents of the lunar crust. The remainder of the text addresses processing of materials, particularly the need for separation of feedstock minerals. To illustrate this need, the text includes descriptions of two norite feedstocks for lunar simulants: the Stillwater Complex in Montana, United States, and the Bushveld Complex in South Africa. Magnetic mineral separations, completed by Hazen Research, Inc. and Eriez Manufacturing Co. for the simulant task, are discussed.					
15. SUBJECT TERMS lunar regolith simulant, mineral separates, in situ resource utilization, lunar minerals, feedstock, rock classification					
16. SECURITY CLASSIFICATION OF:			17. LIMITATION OF ABSTRACT	18. NUMBER OF PAGES	19a. NAME OF RESPONSIBLE PERSON
a. REPORT	b. ABSTRACT	c. THIS PAGE			STI Help Desk at email: help@sti.nasa.gov
U	U	U	UU	60	19b. TELEPHONE NUMBER (Include area code) STI Help Desk at: 443-757-5802



National Aeronautics and  
Space Administration  
IS20

**George C. Marshall Space Flight Center**  
Marshall Space Flight Center, Alabama  
35812